URTeC: 3723724

Production Analysis and Production Forecasting in Unconventional Reservoirs Using Initial Production Data

Oladapo Adejare*[1], Darryl Tompkins[1], Marci Kerls[1] 1. Revo Testing Technologies.

Copyright 2022, Unconventional Resources Technology Conference (URTeC) DOI 10.15530/urtec-2022-3723724

This paper was prepared for presentation at the Unconventional Resources Technology Conference held in Houston, Texas, USA, 20-22 June 2022.

The URTeC Technical Program Committee accepted this presentation on the basis of information contained in an abstract submitted by the author(s). The contents of this paper have not been reviewed by URTeC and URTeC does not warrant the accuracy, reliability, or timeliness of any information herein. All information is the responsibility of and is subject to corrections by the author(s). Any person or entity that relies on any information obtained from this paper does so at their own risk. The information herein does not necessarily reflect any position of URTeC. Any reproduction, distribution, or storage of any part of this paper by anyone other than the author without the written consent of URTeC is prohibited.

Abstract

Rate transient analysis ("RTA") is used to determine fracture and reservoir parameters and well geometries in unconventional reservoirs. It is applied to production forecasting, evaluating completion effectiveness, type well construction and well spacing optimization. Choke management and data quality during the initial production period (i.e., within the first two months of a well's life) has been recognized as crucial to optimizing well performance in unconventional reservoirs and in the early determination of completion effectiveness. This paper illustrates the additional significance of the initial production period by showing how model matches to initial production data are used to seed models for EUR estimation.

Linear flow analysis is one of the most common methods for analyzing well performance in unconventional reservoirs. One of the key insights presented in this paper is that accurate, hourly, automated measurements that preserve reservoir transients indicate that fracture interference may be occurring earlier than suggested in linear flow analysis. Fracture interference was identified with hourly data on Log-Log plots of Rate Normalized Pressure ("RNP") vs. Material Balance Time ("MBT") and Flowing Material Balance ("FMB") plots generated from numerical models and field data. Numerical models were used to test and validate well geometry assumptions indicating early interference for single and multifracture examples and then the workflow was applied to wells in the SPE Data Repository.

Fracture and reservoir parameters determined from analysis of initial production data adequately seeded models for an oil well and a gas well in the SPE data repository. The model match using the fracture half-length and permeability from the initial production period started to over predict cumulative production when a unit slope was observed on flow regime identification plots. The model matched the data when constrained by the contacted volume for each well, indicating that the analysis method can be accurate when boundaries are defined and can help identify the magnitude of lost performance if the fracture half-length and permeability degrade, or interference occurs. This workflow has now been applied to hundreds of wells across multiple unconventional basins in the US.

Early fracture interference has been proposed previously, but to the authors' knowledge this is the first time it has been demonstrated using hourly initial production data. The reservoir transients that may indicate earlier facture interference are masked by lower resolution daily data and low-quality hourly data

with measurement errors. This paper illustrates the additional significance of high frequency/high quality initial production data by showing that the facture half-length, permeability, and number of dominant fractures determined within the first 2 months of production are representative of performance until interference occurs or performance starts to degrade.

Introduction

RTA is used to determine completion and reservoir parameters and to define the geometry of wells in unconventional reservoirs. Example applications are in production forecasting (P.W. Collins, 2015, Anderson, et al., 2010), creating type wells (Alexander C. Eleiott, 2019, Lemoine & Lee, 2019, Ravikumar & Lee, 2020, Sukumar & Lee, 2019) matching and forecasting data using type curves (Nobakht, Clarkson, & Kaviani, 2011) and in well spacing studies (Burget, et al., 2021, Aniemena, et al., 2019). Using rate and pressure data in the analysis (as opposed to rate alone in decline curve analysis) can provide additional insights because it can account for changing operating conditions as well as estimate original fluids in place, drainage area, recovery factors, and permeability and skin/fracture half-length for evaluating completion effectiveness.

The most common method for analyzing production data using rate transient analysis in unconventional reservoirs is based on the analysis of a linear flow regime as observed on a log-log plot of RNP vs. MBT (Olivier Houze, 2021) in Figure 1. The linear flow regime is followed by fracture interference and finally flow into the stimulated reservoir volume ("SRV") for unbounded wells.

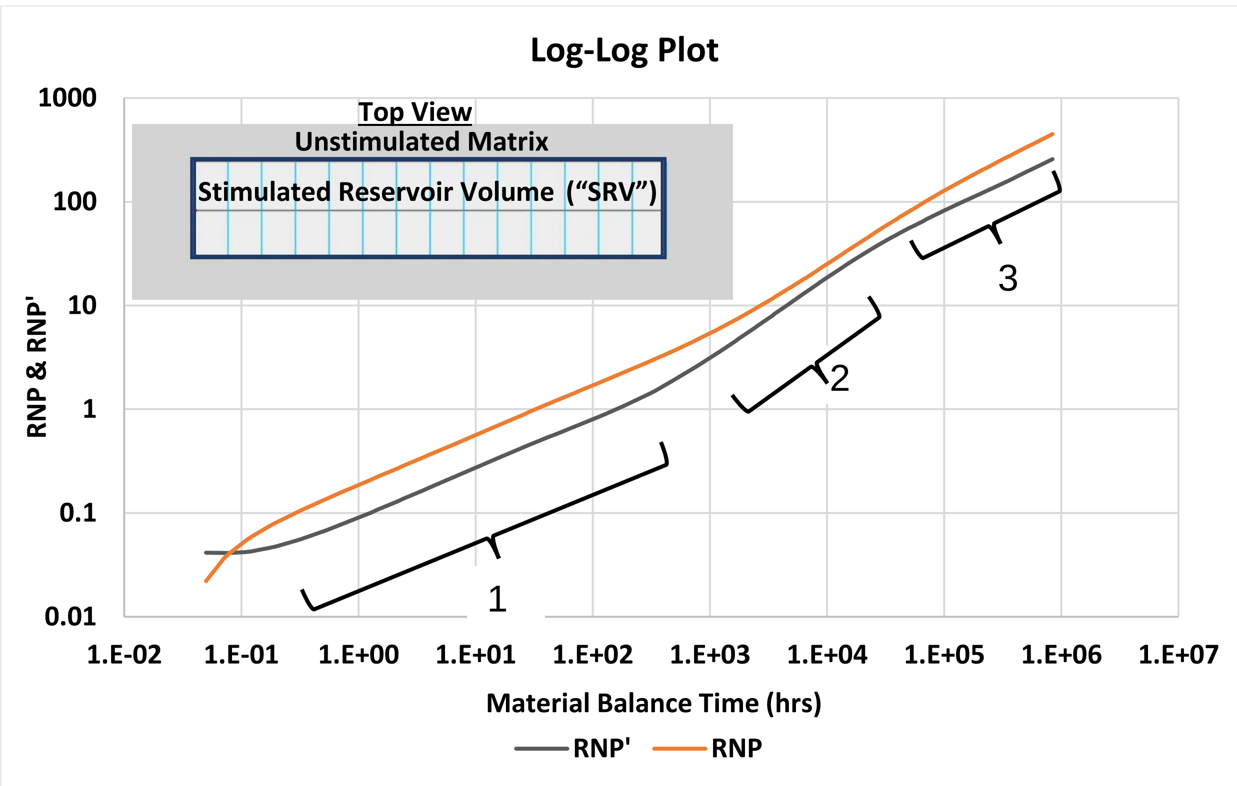

Figure 1 - Expected flow regimes for SRV bounded wells: 1. Linear flow into fractures 2. SRV Bounded Flow 3. Linear flow into SRV

When fluid PVT properties and saturations are not changing significantly a plot of RNP vs. sqrt MBT (figure 2) for an oil well in linear flow will have the slope proportional to the lumped parameter term

"$n \times x_f \times h \times \sqrt{k}$" which is a combination of the number of stages (n, for a horizontal well with multiple transverse fractures), fracture half-length (xf, ft.), height (h, ft.), and permeability (k, md.) .

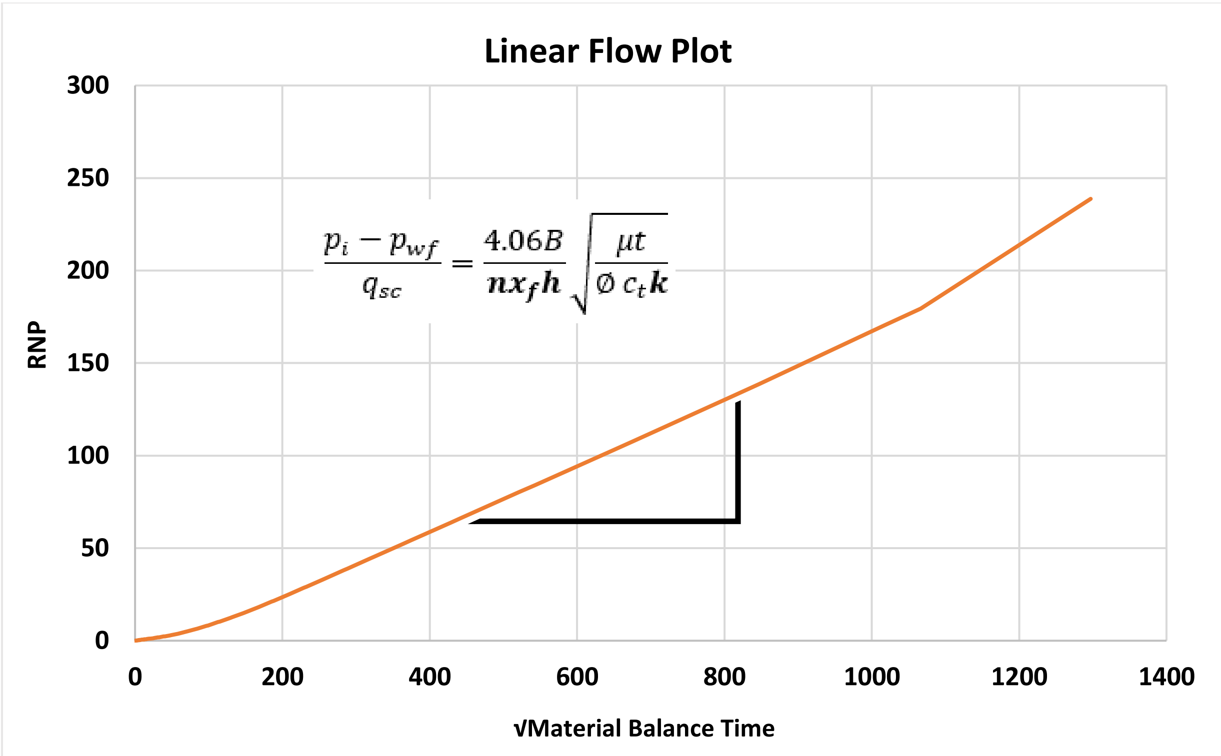

Figure 2 - Linear flow plot and equation for calculating fracture half length, number of stages and permeability (Olivier Houze, 2021). P is pressure in psi (subscript "i" is for initial and "wf" is for flowing pressure), q_{sc} is the rate in bbl./day, B is the formation volume factor (RB/STB), u is viscosity (cp), t is time (hours), Ø is porosity and c_t is the total compressibility (1/psi)

The number of fractures, permeability, and fracture half-length can be calculated when the volume of the SRV is known. However, this match is non-unique. A wide range of permeabilities and fracture half lengths can match the data. One way the solution can been constrained is with an independent estimate of permeability obtained from a diagnostic fracture injection test ("DFIT"). However, permeabilities derived from DFITs can vary over a wide range depending on the analysis methodology used for interpretation. Fowler, et al. (2019) estimate a lower permeability from DFITs, in contrast with, Barree, et al. (2015) that report larger values of permeability from their DFIT analysis.

In addition, Barree, et al. (2015) also estimate permeability uniquely from RTA with a flow regime sequence where fracture interference precedes channel flow and is then followed by the outer (well to well or SRV) boundary. This suggests earlier fracture interference than indicated by the linear flow regime sequence where fracture interference coincides with the SRV or well to well boundary as shown in Figure 1.

This paper presents observations from initial production data supporting the early fracture interference flow regime sequence. Furthermore, it will show how permeability, fracture half-length, number of dominant fractures, cluster efficiency and fracture spacing can be estimated from the initial production period (usually within the first two months of production) and used to seed models to forecast production for wells exhibiting a unit slope in flow regime identification plots. It builds on earlier work (Crafton, 1998) where the fracture half-length and reservoir permeability determined at the end of flowback for hydraulically fractured wells was used in evaluating completion effectiveness.

Theory and/or Methods

Recent studies from fracturing test sites have provided invaluable data and observations. In order to develop the modelling approach presented here, observations with respect to fracture characterizations from slant core, microseismic, mug logging, and offset pressure monitoring were considered. What has been adopted into the model presented in this paper are smooth, parallel fractures with increasing fracture / proppant density close to the wellbore and far field drainage facilitated through the presence of a relatively small number (1-2 per stage) of principal or "mother" fractures (Raterman et. al. 2020, Bessa, et al., 2021). A simplified schematic is shown in Figure 3 below.

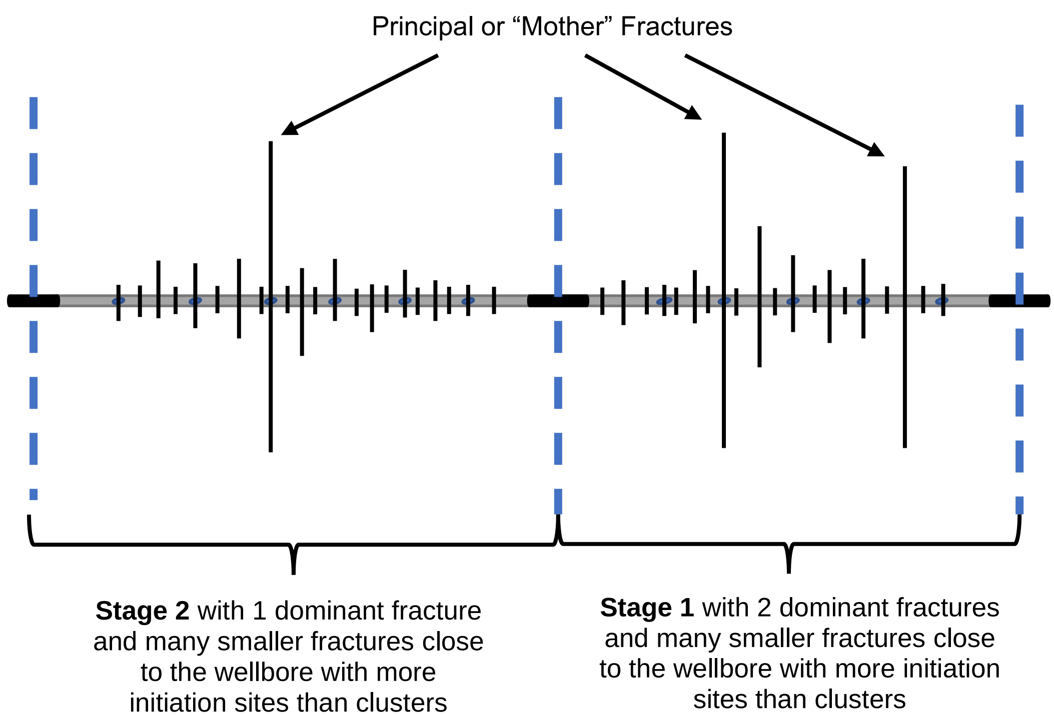

Figure 3 - Interpretation of basic fracture distribution and geometry from hydraulic fracturing test sites

When this interpretation of fracture distribution and geometry is applied to a numerical model the following flow regime sequence indicating early fracture interference can be obtained:

1. Early linear / interstage fracture interference (slope of 0.5 or less)
2. Boundary between stages / dominant fractures (unit slope)
3. Linear channel flow (0.5 < slope< 1)
4. Boundary between wells (unit slope)

Figure 4 shows the log-log plot generated from the model as well as the model inputs.

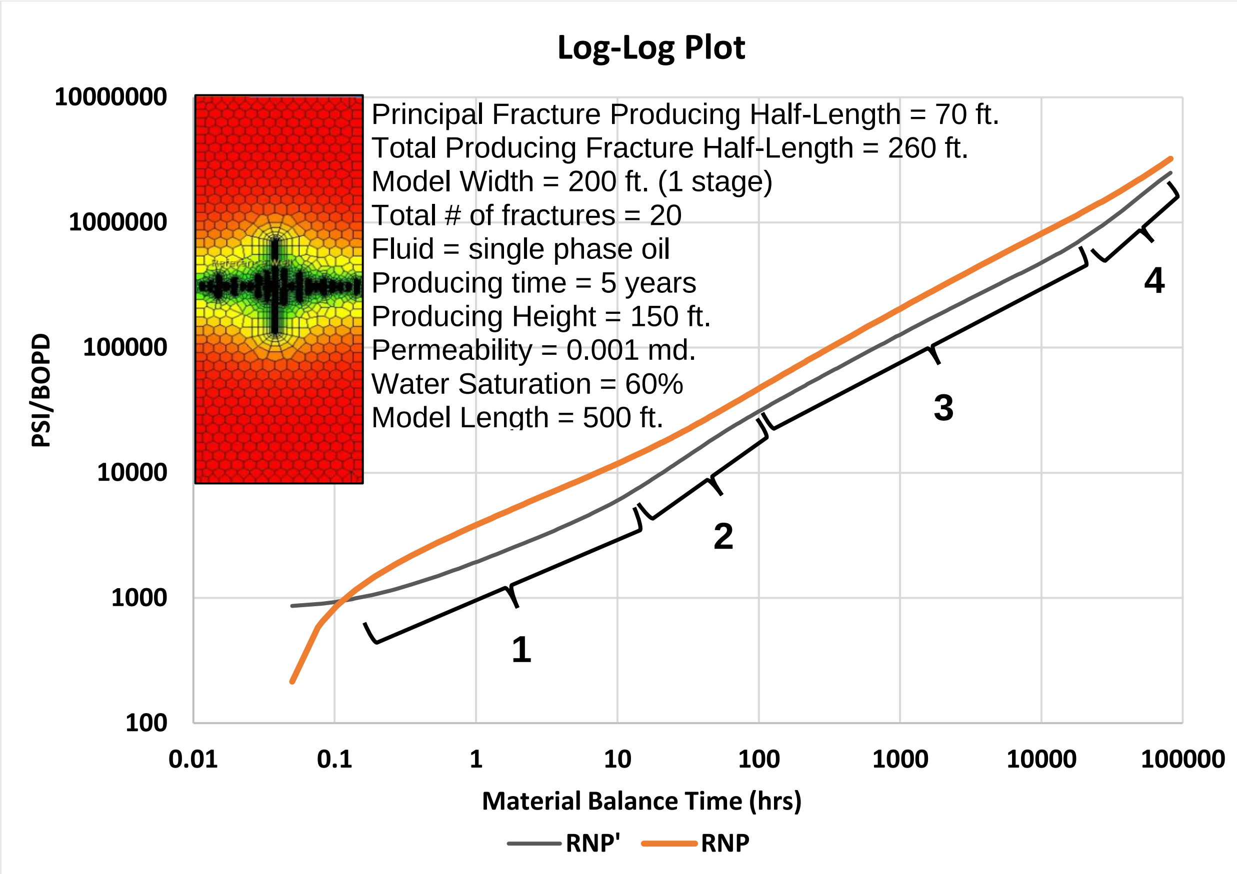

Figure 4 - Log-Log plot showing the model inputs and flow regime sequence for a single stage (1) Early linear / interstage fracture interference (2) Boundary between stages / dominant fractures (3) Linear channel flow (4) SRV or Boundary between wells

Of particular interest here is the identification of the transient encountering the first boundary between stages / dominant fractures. This occurs roughly 20 hours into the test and quite often we will see interference occur within 500 hours (20 days) after the introduction of a transient into the reservoir.

This numerical model and what we have observed in field data suggests that if rate and pressure data is to be used in Rate Transient Analysis, it needs to include all of the data (flowback and production) from the time the well is first opened, and the data must be of sufficient quality to be analyzed with confidence. If flowback/initial production data is not included or it is not of sufficient quality, it can lead to the misinterpretation of linear channel flow as fracture linear flow which would lead to the misinterpretation of permeability (much lower) and fracture half-length (much higher).

Next, a simplified analytical model is created to approximate the behavior observed in the numerical model. Figure 5 shows the simplified model with each flow regime that will be analyzed to seed more complex analytical and numerical models. The simplified flow regime sequence is as follows:

1. Early intra stage fracture interference – this usually happens in the first 10-50 hours and in our experience flow regimes can be difficult (if not impossible) to see during this period.
2. Boundary between stages/dominant fractures – this usually occurs between 50-500 hours and could be longer for gas wells.
3. Linear channel flow – This is the dominant flow regime we see on most tests and often has a slope on the log-log derivative greater than 0.5 (linear flow) but less than 1 (boundary dominated flow).

4. Fully bounded flow – Contact with this boundary usually occurs a year or later into the producing life of the well due to interference between offset wells. However, we have seen it occur early if offsets are very close, there is direct communication between wells, or the well has been damaged. If there are no offsets this flow regime would be followed by linear flow into the SRV or late time pseudo radial.

The simplified model makes a consistent interpretation of interference and determination of fracture and reservoir parameters possible as shown in the next section.

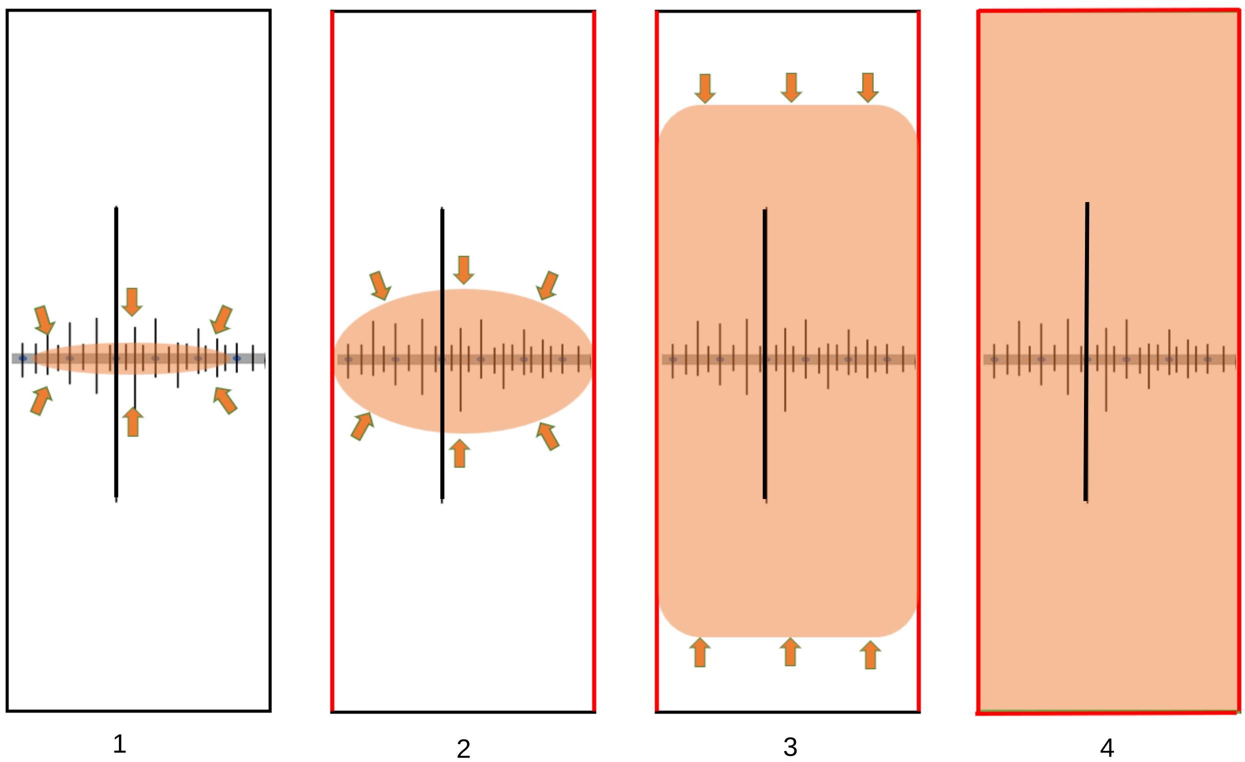

Figure 5 - Simplified model with flow regime sequence (1) Early intra stage fracture interference (2) Boundary between stages/dominant fractures (3) Linear channel flow (4) Fully bounded flow

Identifying the Boundary Between Dominant Fractures with Hourly Data

Figure 6 shows a production history plot of two wells (A and B) completed next to each other in 2019 in the Eagle Ford formation of South Texas. This is a typical example of what can be seen when accurately measured hourly rates and pressures that preserve reservoir transients are compared with less accurate measurements where measurement errors mask reservoir transients. Well A was flowed through a fully automated testing system with high measurement quality. Every choke change is accompanied by a consistent rate increase and the data is smooth (minimal rate fluctuations) in-between choke changes. In contrast for well B there are significant rate fluctuations in-between choke changes caused by measurement errors.

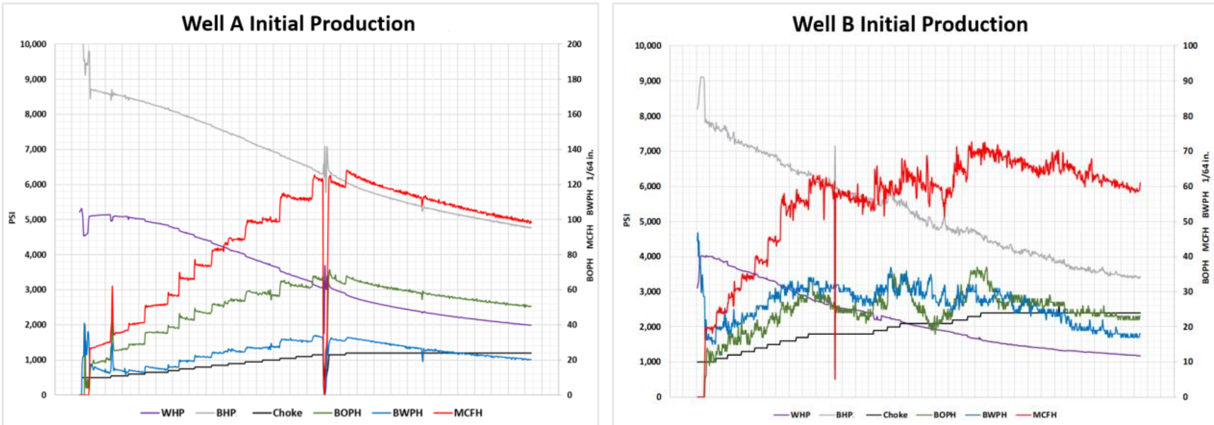

Figure 6 - Initial Production (flowback) History Plot with engineered flowback and superior data quality (Well A) and poor data quality (Well B)

The following observations can be made when data from Well A in Figure 6, which uses hourly, automated, accurate measurements is plotted on a normalized rate cumulative plot in Figure 7.

1. The slope associated with each choke change can be seen on the normalized rate cumulative plot (indicated by black lines).
2. The right-ward shift in the horizontal intercept indicates that with each choke increase the contacted volume increases.
3. When the choke is held for a week at the end of the test, the slope is initially unchanged, and then starts to get shallower after a few days. This implies that holding the choke for a week allowed sufficient time for the transient from each dominant fracture to propagate and start to interfere with other fractures, as illustrated in step 2 of Figure 5.

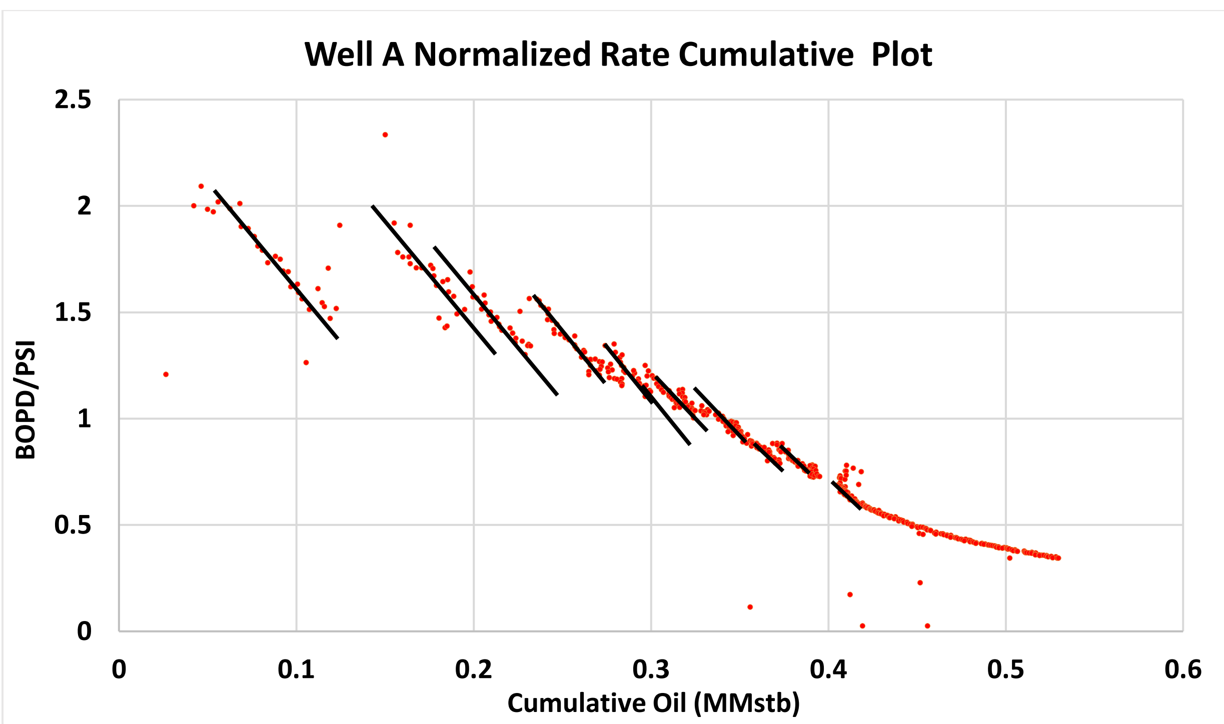

Figure 7 - Transients associated with each choke change in Well A are visible with good data quality

The time to fracture interference was about 80 hours based on the time from the last choke change to the inflection on the derivative of the log-log plot in Figure 8. The inflection precedes the start of channel flow. We infer from Figure 8 that when choke changes were being made every 12-24 hours there wasn't sufficient time for the transient to propagate far enough for interference to occur.

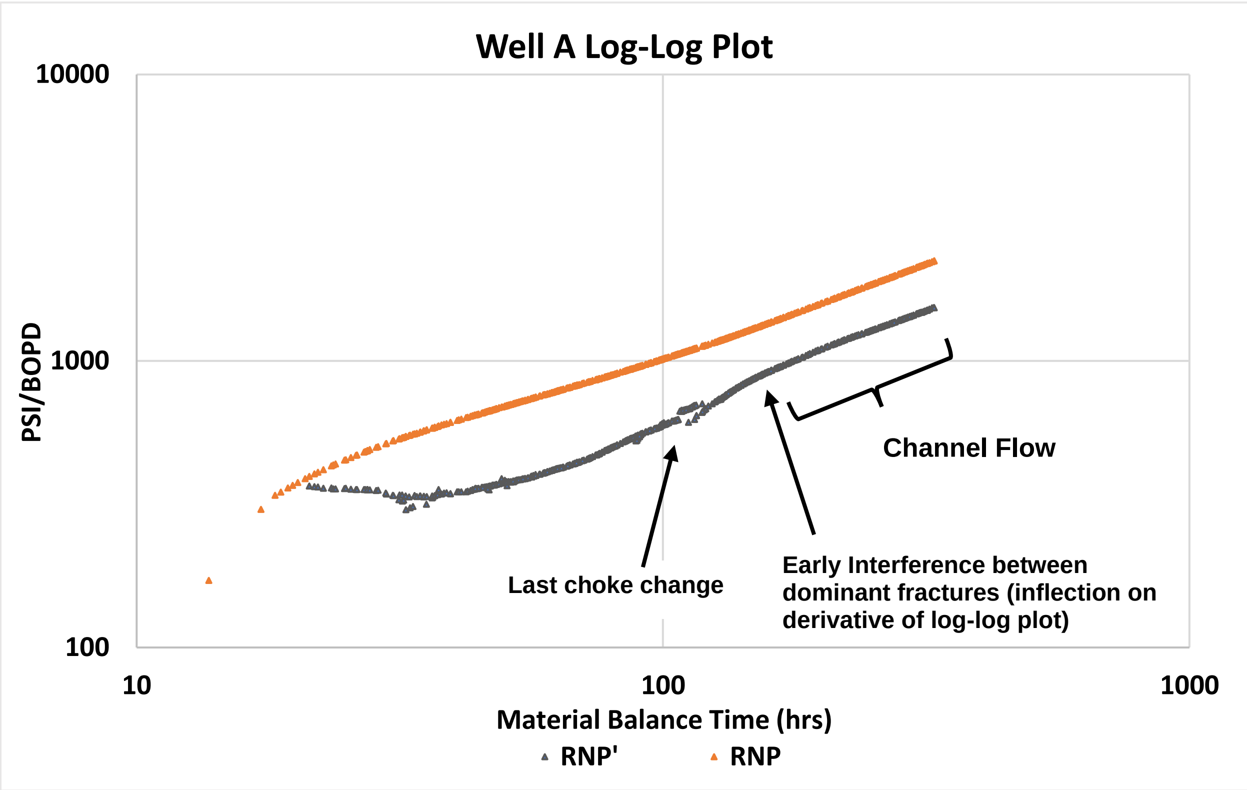

Figure 8 - The Log-Log Plot of initial production data for Well A shows an inflection on the derivative indicative of interference between stages / dominant fractures. This can only be seen with accurate hourly rate and pressure measurements.

This trend has been observed by the authors in oil and gas wells in all unconventional reservoirs in the United States when accurately measured hourly rates and pressures and choke data are available.

In contrast when data quality is poor the transients created by each choke change (Well B) cannot be seen (Figure 9). While the decrease in slope at the end of the test is apparent, it is not clear if the frequency of choke changes had an influence in preventing the propagation of the transient.

The boundary between dominant fractures / stages can be nearly impossible to see if the data quality is poor, which is often the case with initial production data (flowback data), as demonstrated in the log-log plot for Well B in Figure 10. When compared to Well A (Figure 8), the fluctuations on the derivative of the log-log plot for Well B indicate there were significant rate measurement errors masking the reservoir transients. Rate changes did not coincide with choke changes and the inflection signature for early interference on the derivative of the log-log plot is not clearly visible.

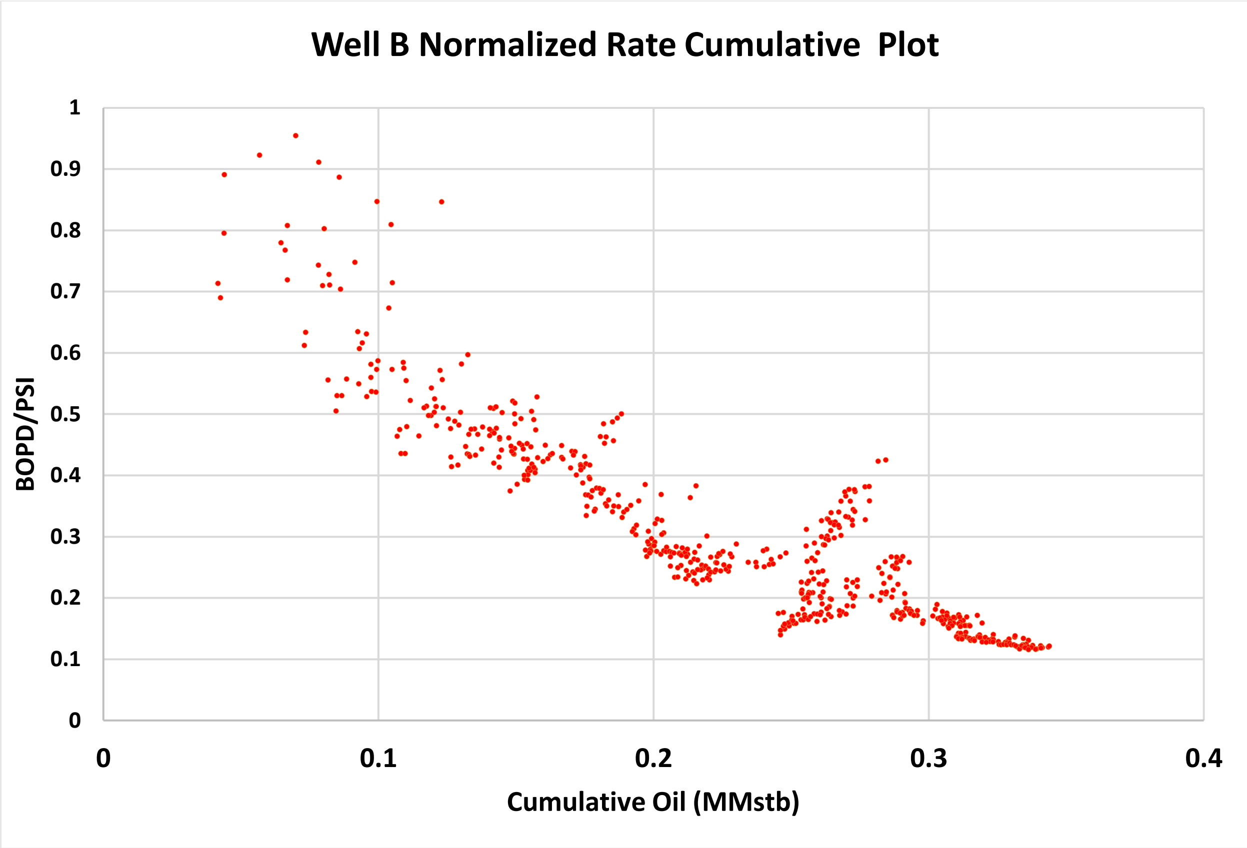

Figure 9 - Individual transients associated with each choke change cannot be seen because data quality is poor

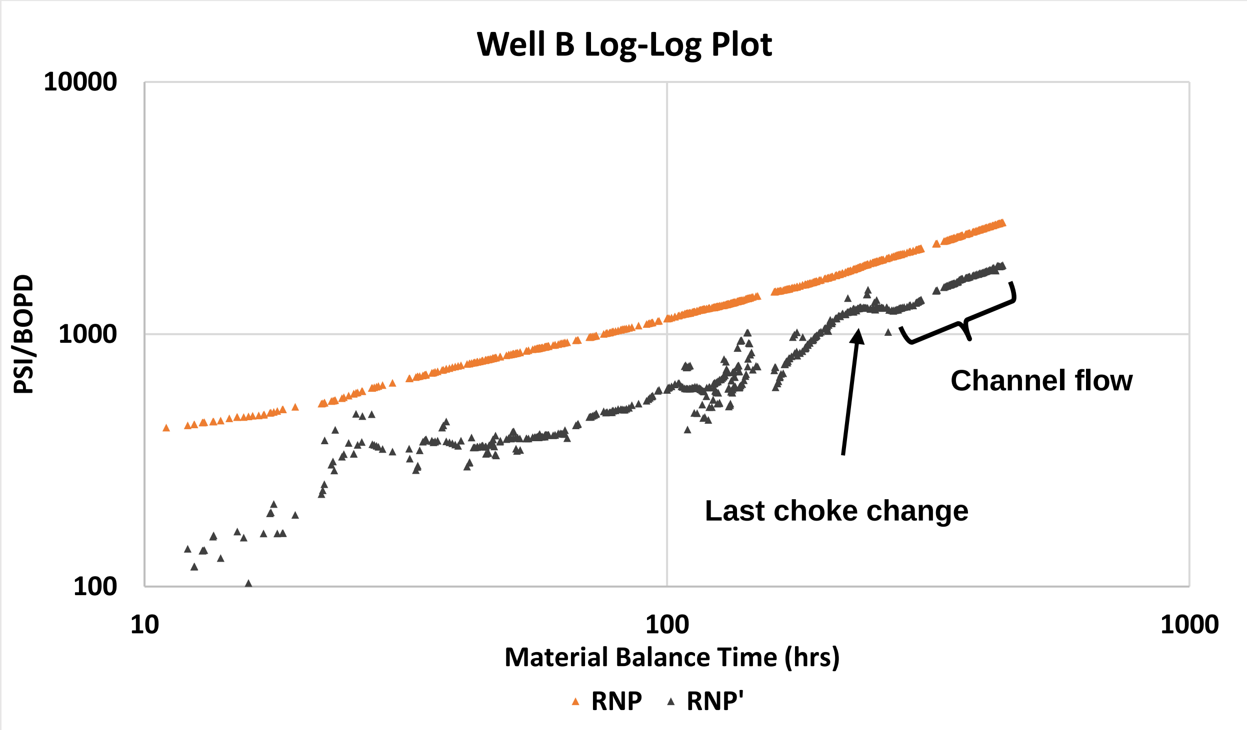

Figure 10 - Log-Log Plot for horizontal Eagle Ford well that shows how rate errors masks the inflection on the derivative indicative of the interference between dominant fractures.

Every effort should be made to collect the best quality data from the first day the well is opened (Tompkins et. al. 2020). In addition to ensuring the best data quality it is advised to use an engineered drawdown strategy early in the well's life to minimize damage that can be caused to completions by aggressive drawdown strategies (Crafton, 2008; Okouma, et al., 2011; Deen, et al., 2015; Tompkins, et al., 2016; Rojas & Lerza, 2018; Lerza, et al., 2018; Belyadi, et al., 2016; Alzahabi, et al., 2021). We have found that when a controlled drawdown is combined with good data quality during flowback, identification of the first boundary is much easier.

Model Validation

Numerical Model (1 stage)

To better understand the simplified model, a single-phase gas numerical model was created with the properties shown in Table 1 and run at a constant rate for 1 year.

Model Inputs	
Fracture Half length (ft)	40
Fracture Height (ft)	100
Initial Reservoir Pressure (psi)	7,000
Permeability (md)	0.001
Porosity (fraction)	0.1

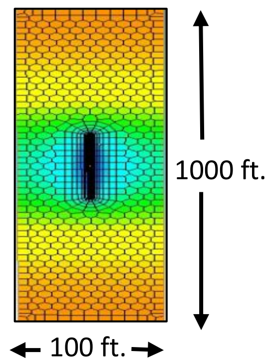

Table 1 - Model inputs for single fracture Numerical model

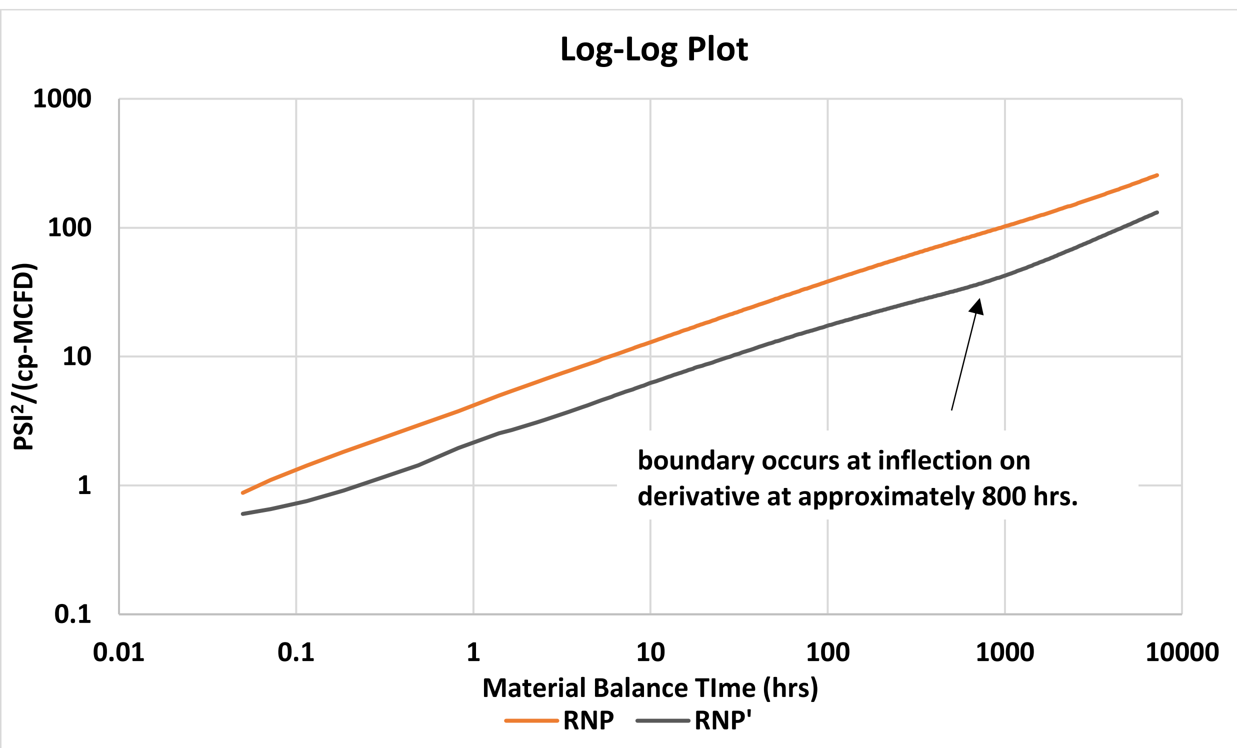

Figure 11 - Log-Log plot for single phase gas model showing early interference

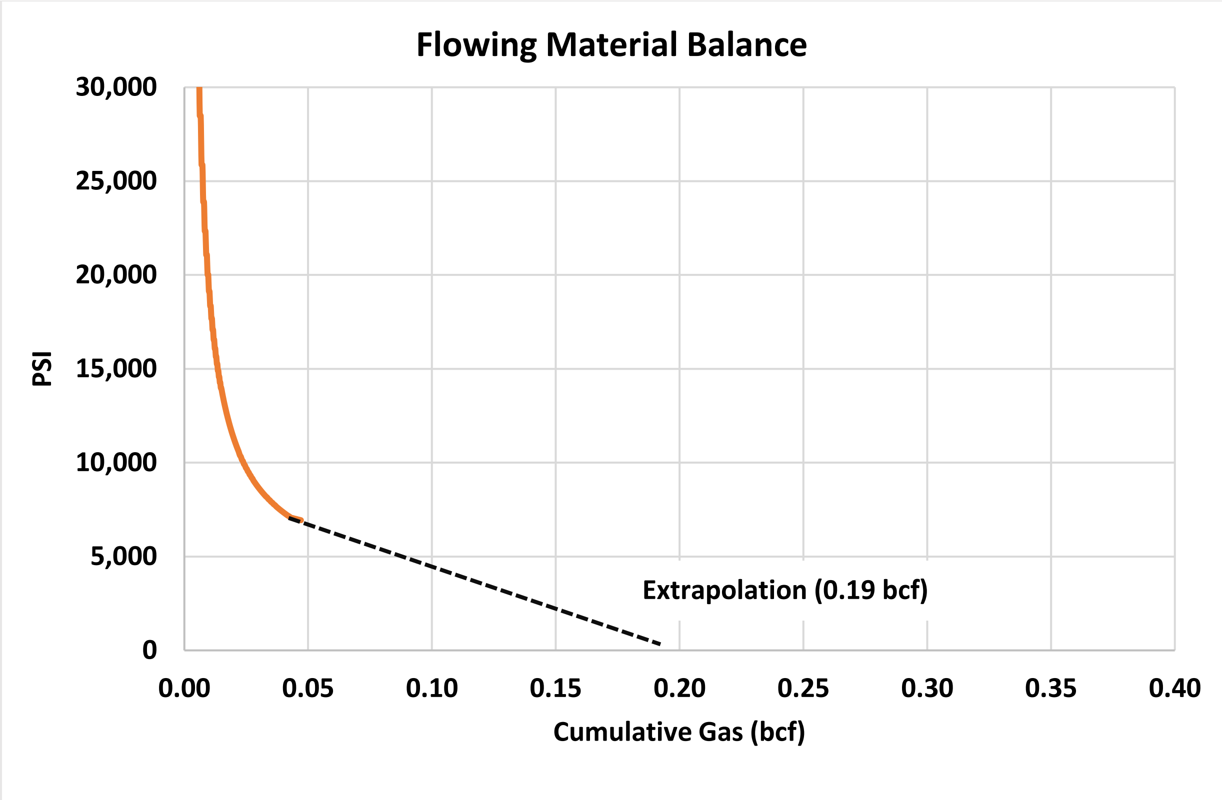

Figure 12 – FMB plot indicating volume at first boundary

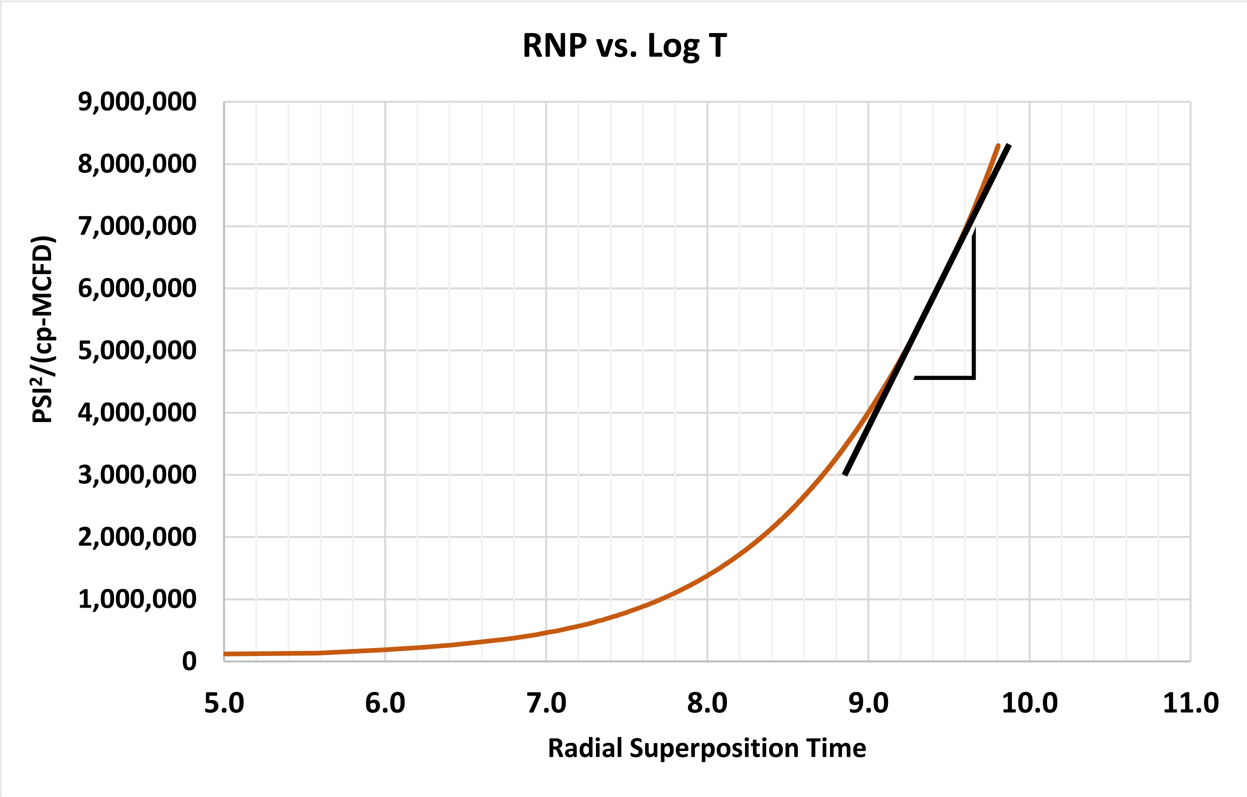

Figure 13 - Slope (black line) to the data from which permeability and fracture half-length are calculated. The solution assumes radial flow as defined by Lee, et al. (2003)

Similar to the accurately measured hourly data from Well A in Figure 8, early fracture interference occurred at around 800 hours based on the inflection in the derivative of the log-log plot (Figure 11).

An extrapolation to the trend on the FMB plot coinciding with the start of fracture interference gives a volume of 0.19 bcf (Figure 12). Finally, model match to the data just before the first boundary (similar to Barree, et al., 2015) assuming radial flow gives a permeability of 0.001 md and fracture half-length of 40 ft. consistent with the model (Figure 13).

Justification for Radial Flow and Short Fracture Half-Length

Numerical experiments with the single fracture model boundaries indicate that the analysis would only determine the correct fracture half-length and permeability when the fracture half-length is less than half the distance between dominant fractures implying generally shorter fracture half-lengths from the analysis compared with what is typically reported.

A justification for short fractures is provided in Barree (2019) and Barree, et al. (2019). Fractures are initially 100% water saturated at the start of flowback. Fracture cleanup is controlled by the relationship between viscous forces (drawdown at the wellbore) and capillary forces resisting displacement of water by hydrocarbons. Pressure gradients across a fracture were calculated for a fracture flowing at typical rates for the initial production period and found to be less than the gravity or buoyancy force at relatively short distances from the wellbore so that clean-up is dominated by capillary and gravity forces.

Capillary and gravity dominated cleanup appears consistent with low fluid recovery in unconventional wells. This would result in relatively shorter effective fracture half-lengths compared to the created or propped lengths as illustrated in Figure 4.

Numerical Model Validation (100 stages)

Next the analysis is done for a horizontal well flowing single-phase gas with equally spaced multiple transverse fractures with inputs in Table 2. This example illustrates how the fracture half-length; permeability and the number of dominant fractures is determined for wells with multiple transverse fractures.

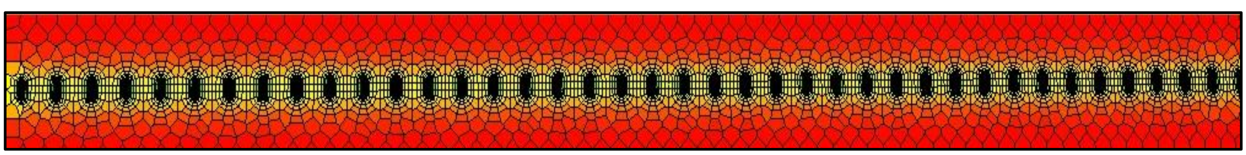

Model Inputs			
Fracture Half length (ft)	40	Permeability (md)	0.001
Number of fractures	100	Porosity (fraction)	0.1
Fracture Height (ft)	100	Lateral Length (ft)	10,000
Initial Reeservoir Pressure (psi)	7,000		

Table 2 - Numerical model with multiple transverse fractures (top) and model inputs (bottom)

Similar to accurately measured hourly data from Well A in Figure 8, fracture interference is determined from the inflection on the derivative of the log-log plot (Figure 14). An extrapolation of the data at that same time on the normalized rate cumulative plot gives the approximate volume contacted at the time of fracture interference of 2.5 bcf (Figure 15).

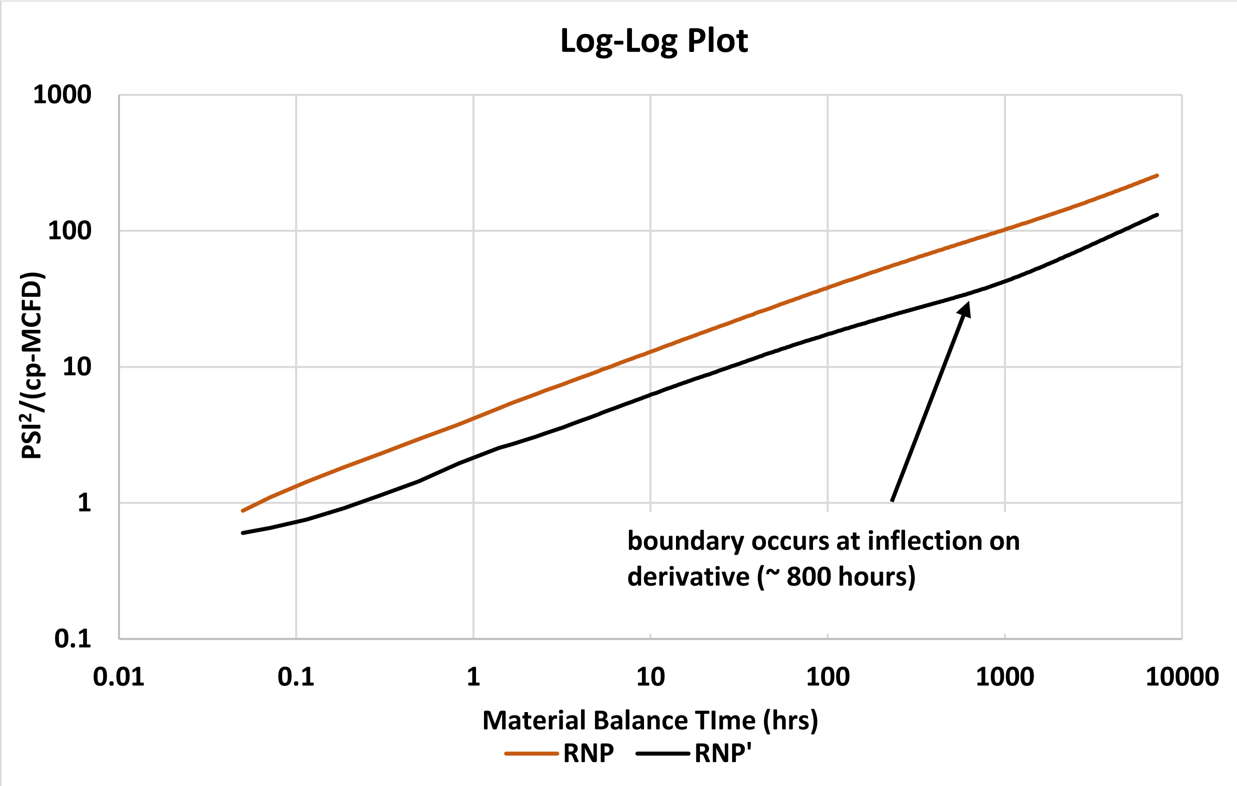

Figure 14 - Flow Regime Analysis showing interference at 800 hours

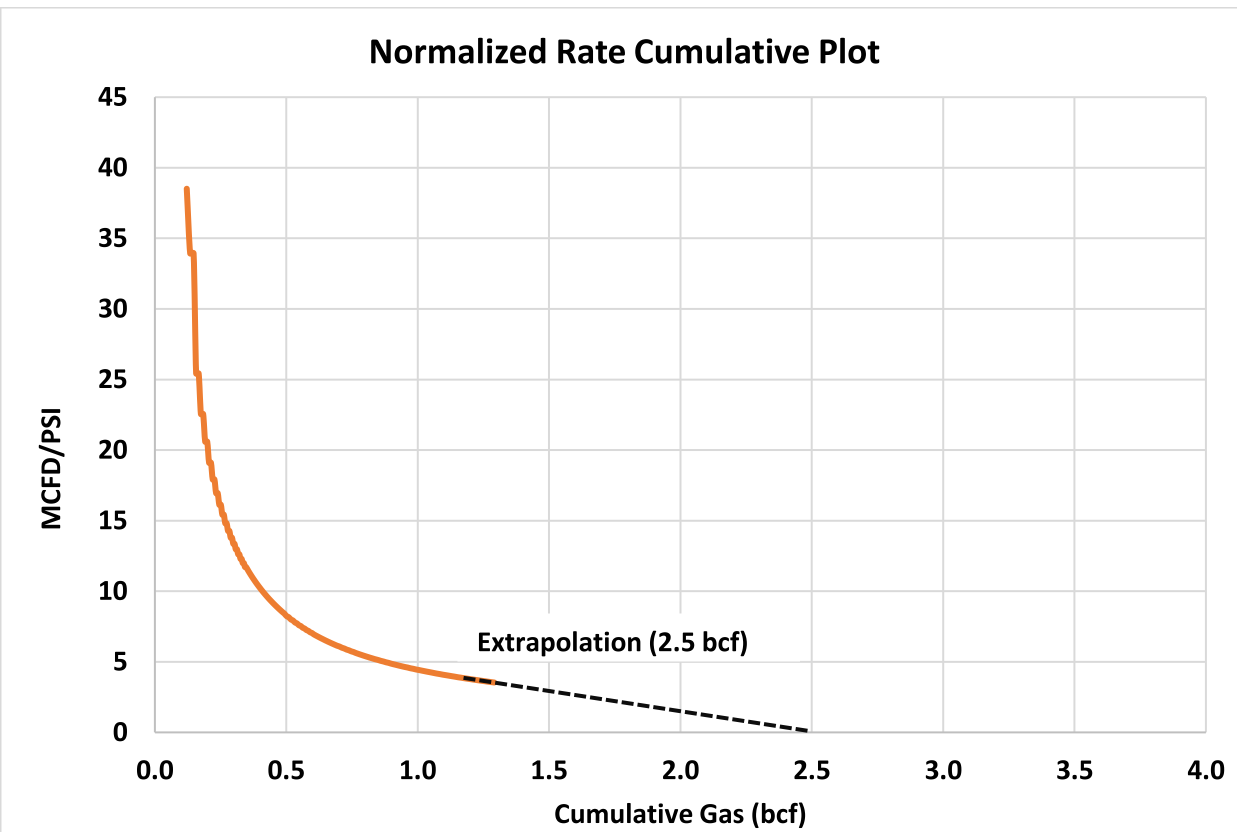

Figure 15 - Volume at interference for multi-stage example

With the volume at fracture interference calculated, the number of stages is calculated as follows (and is summarized in Table 3):

1. Calculate bulk volume using the given porosity, saturation, and initial formation volume factor
2. Estimate the number of fractures contributing (a good initial guess is 1-2 fractures / stage)
3. Calculate distance between dominant fractures (r_{e1}) using $\pi r_e^2 h n_s = Bulk\ Volume$. Where h = producing height of the formation and n_s = number of contributing fractures. This assumes the transient propagates radially from each dominant fracture before fractures start to interfere, and that the volume of interfering fractures is equal to the volume contacted at the first boundary on the flowing material balance plot.
4. Divide the lateral length by the number of fractures to get an estimate of the distance to boundary (r_{e2})
5. Compare values for distance to the boundary in steps 3 and 4. If different, increase or decrease the number of stages till the distance to the boundary converges.
6. Calculate the total system height (height/stage × number of dominant fractures)

Using these steps, 102 fractures were calculated from the analysis in comparison with the actual value of 100 in the model (Table 3). The calculated distance between fractures was 100 ft, again similar to the model inputs. The total height is plugged into the analytical model and a model match to the data just before interference (at dT = 800 hours, similar to Figure 13) indicates the fracture half-length was 36 ft. and permeability was 0.0011 md, which was close to the value of 40 ft and 0.001 md in the model.

Calculations

volume at first boundary	2,500,000,000	scf
Vb	78,750,000	ft3
height/stage	100	ft
# of dominant fractures	102	
re1	49.6	ft
LL	10,000	ft
re2	**49.5**	**ft**
re2-re1	-0.1	ft
Total height	10,200	ft

Table 3 - Iterations to calculate the number of dominant fractures for a multistage example

Results

The workflow described in the previous sections to identify interference between fractures, and determine the number of dominant fractures and the permeability and fracture half-length is applied to the following field cases from the SPE Data Repository:

1. Gas example (Berg 53)
2. Oil example (Berg 4)

Gas Example (Berg 53)

Well 53 in the SPE Data repository (BERG) is an unbounded horizontal well in the Upper Marcellus in Pennsylvania fractured with 7 stages and 7 clusters/stage. There was 7.5 years of daily rates and pressures available and sand face pressures from the spreadsheet were used as the BHP. Figure 16 shows first 60 days of data which includes the flowback period (first 30 days).

There is no hourly or choke data so individual transients associated with each choke change can't be seen on the contacted volume plot (Figure 17). We have assumed that the last major transient was introduced into the reservoir for Well 53 at 22 days when gas rates start to decline and the inflection occurs in figure 17, though we can't confirm this without choke and hourly data.

In addition, there is an inflection on the derivative of the log-log plot (Figure 18) indicating that fracture interference occurred about 500 hours after the last transient was introduced. This inflection is followed by the start of channel flow (similar to Figure 8,11 and 14).

As demonstrated previously in Figure 12 an extrapolation of the data at 22 days on the FMB plot (Figure 17), indicates 1.09 bcf as the volume contacted at the time of interference between dominant fractures. The iteration to calculate the number of dominant fractures results in an estimated 7 fractures/stage (96% cluster efficiency) and a total height of 10,500 ft and a dominant fracture spacing of 100 ft/fracture (Table 4).

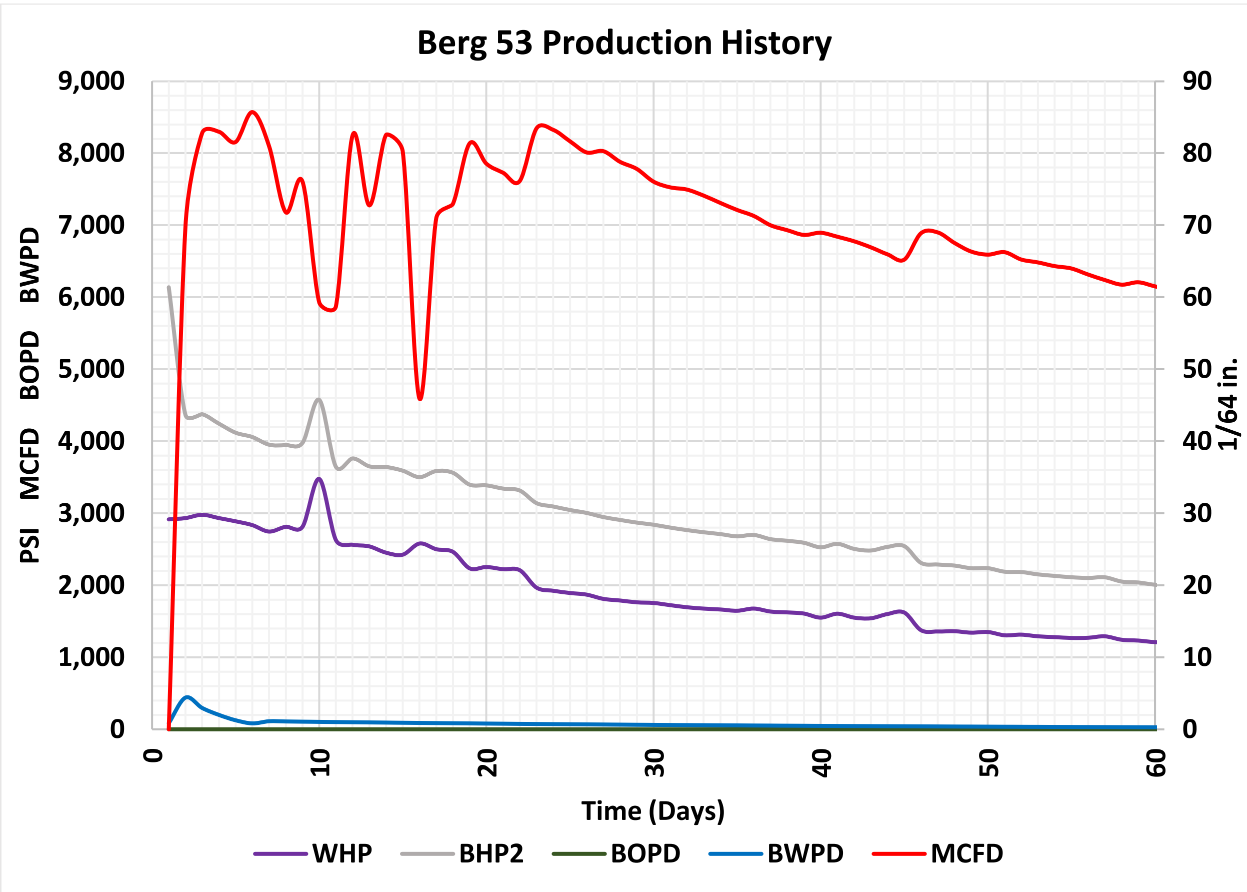

Figure 16 - Initial Production (flowback) of Berg 53

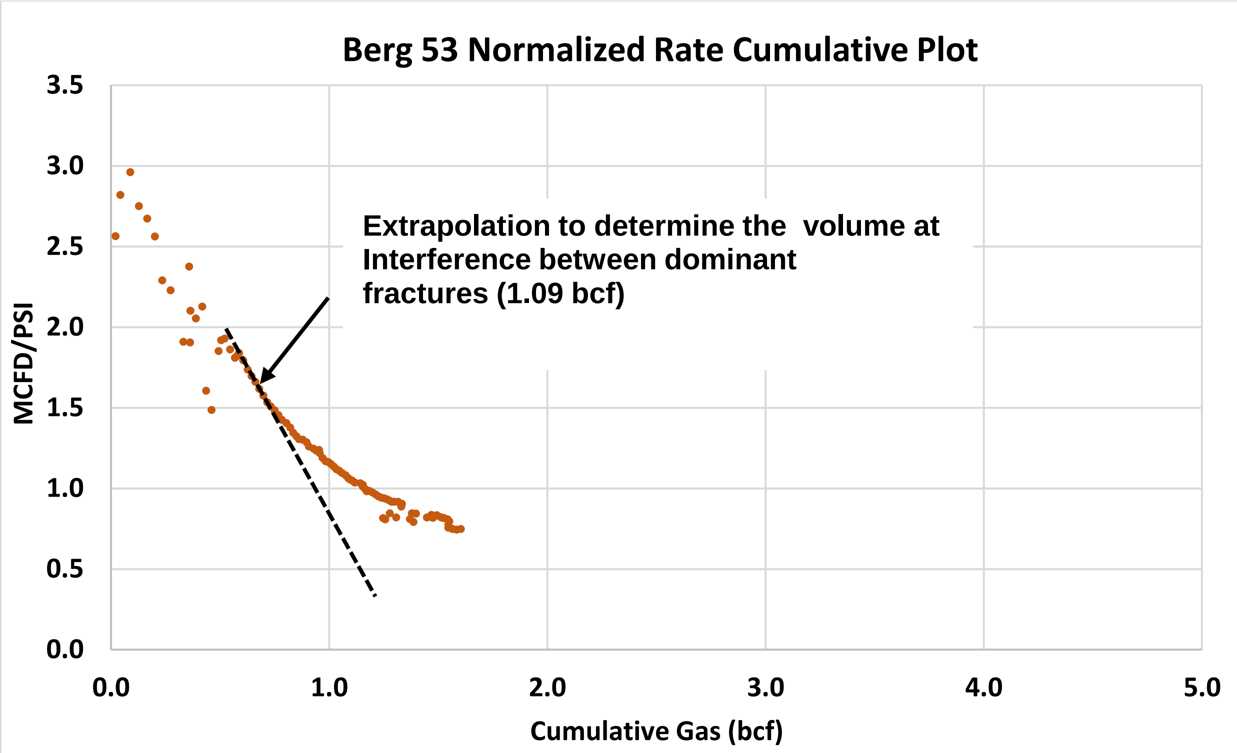

Figure 17 - Extrapolation for volume between dominant fracture / stages with daily data. In contrast with Figure 7 transients for choke changes are not visible

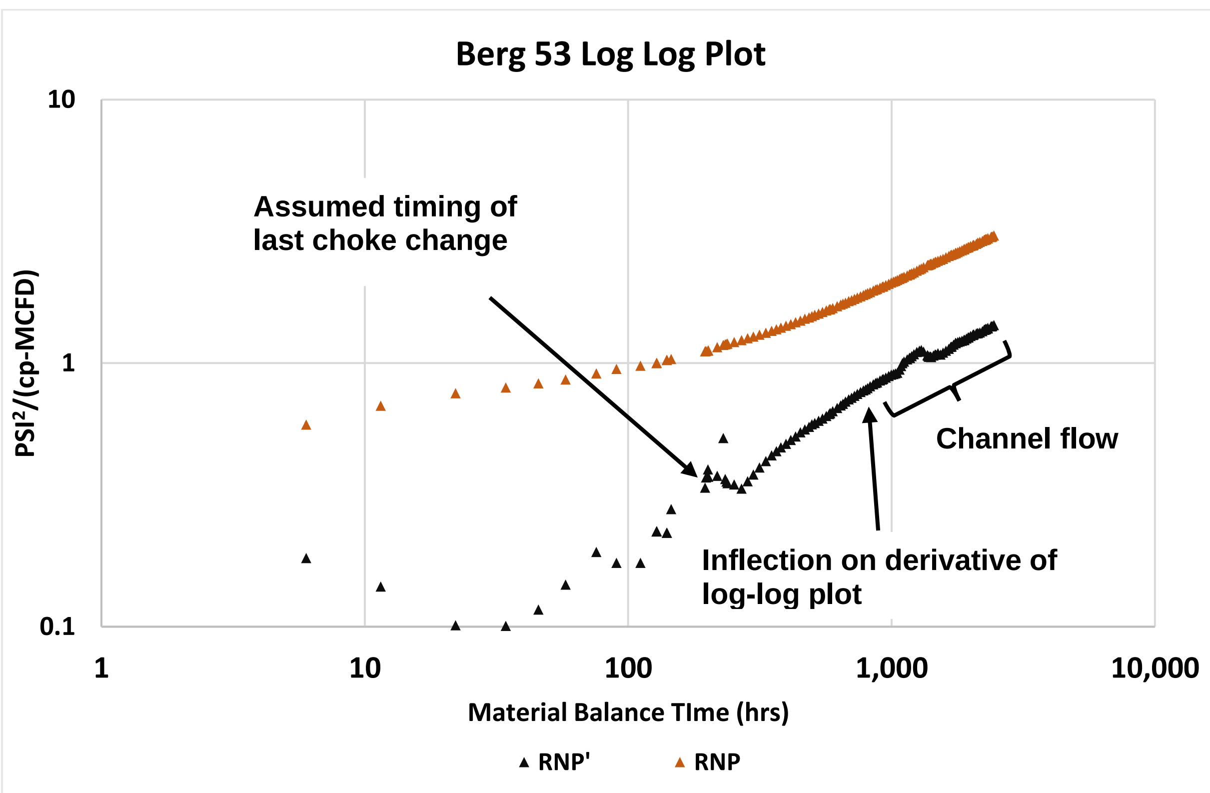

Figure 18 - Log-log plot of initial production (first 22 days) data for Berg 53H

Calculations

Volume at first boundary	1,090,000,000	scf
Vb (Bulk volume)	87,903,226	ft3
height/stage	223.4	ft
# of dominant fractures	47	
re1	51.6	ft
LL	4,744	ft
re2	**51.6**	**ft**
re2-re1	0	ft
Total height	10,500	ft

Table 4 - Calculation of cluster efficiency and number of dominant fractures for Berg 53

Using the total height, a radial flow model match to the data at 30 days, just after interference between dominant fractures (similar to Figure 13 above) gives a permeability of 0.0004 md and a fracture half-length of 40 ft. Seeding the analytical model with this data and adjusting for a better match resulted in a permeability of 0.00045 md and a fracture half-length of 50 ft matching the data with a fracture spacing of 120 ft. Figure 19 and 20 compare the model and data on a log-log and production history plot for the initial production period.

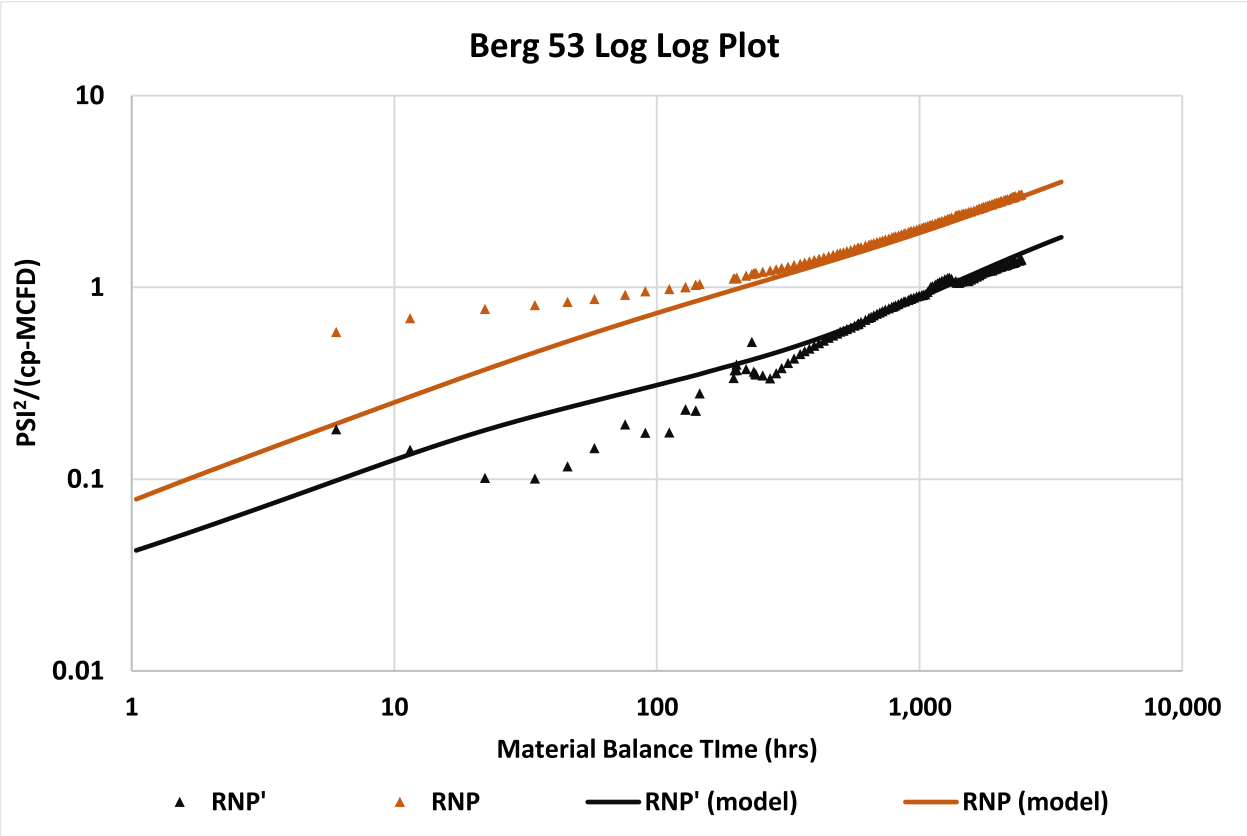

Figure 19 – Log-Log plot of model match to data

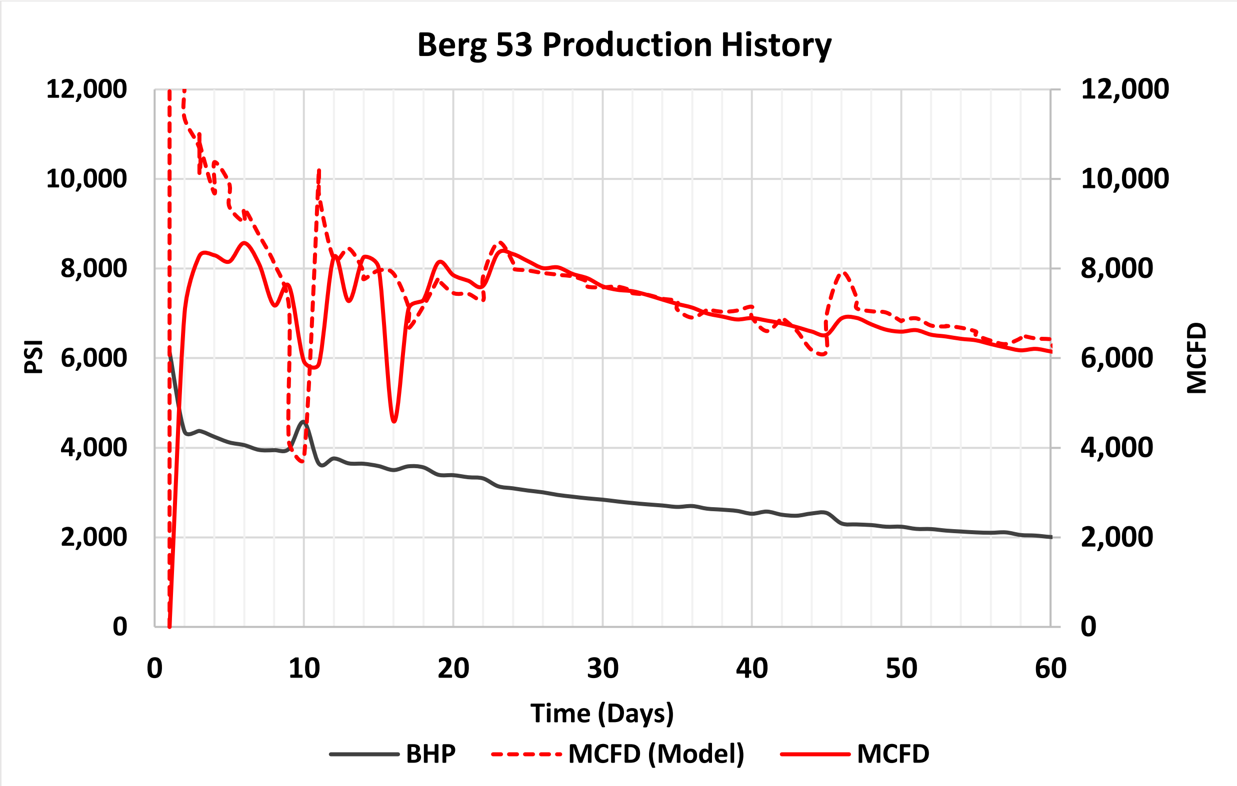

Figure 20 - Model match production history to first 2 months of data with the fracture half-length and permeability determined from initial production.

The fracture and reservoir parameters determined from the model match to the first 60 days of production (Figure 20) are then used to predict production for the next 5 years assuming the SRV extends 500 ft from the wellbore and using the BHP decline in the data set (Figure 21).

The modeled cumulative gas matches the data for the first 2 years, after which the cumulative production starts to increase relative to the actual data. The modeled cumulative gas exceeds the data by 2% after 2 years of production and 8% after 5 years.

With nearly 6 years of data (Figure 21), refinements to the well geometry can be made to improve the model match. A review of the flowing material balance plot for all the data indicates a total volume of 5.5 bcf after 6 years (Figure 22). The log-log plot in Figure 23 indicates a unit slop on the derivative that starts 2 years into production. It's good practice to compare this volume with petrophysical inputs for consistency. Inconsistencies may indicate that input heights or saturations may need to be revised (Whitson Academy, 2022). With the total volume known with 6 years of data the distance to the outer boundary can be calculated and added to the model for a much more accurate match. In Figure 24 the model match with the revised boundary is shown on the cumulative volume of the production history plot.

This case study demonstrates how key parameters for the reservoir and completion can be obtained from the initial production data and used to model the entire well history when the distance to the outer boundary is known or can be estimated with a reasonable degree of confidence. Conversely, the boundary seen at 2 years could be caused by damage to the well. It is important to review the entire well history for indications of possible decreases in well performance beyond those expected in the normal course of the well's life. Unfortunately, this level of detail is not available in the BERG data sets.

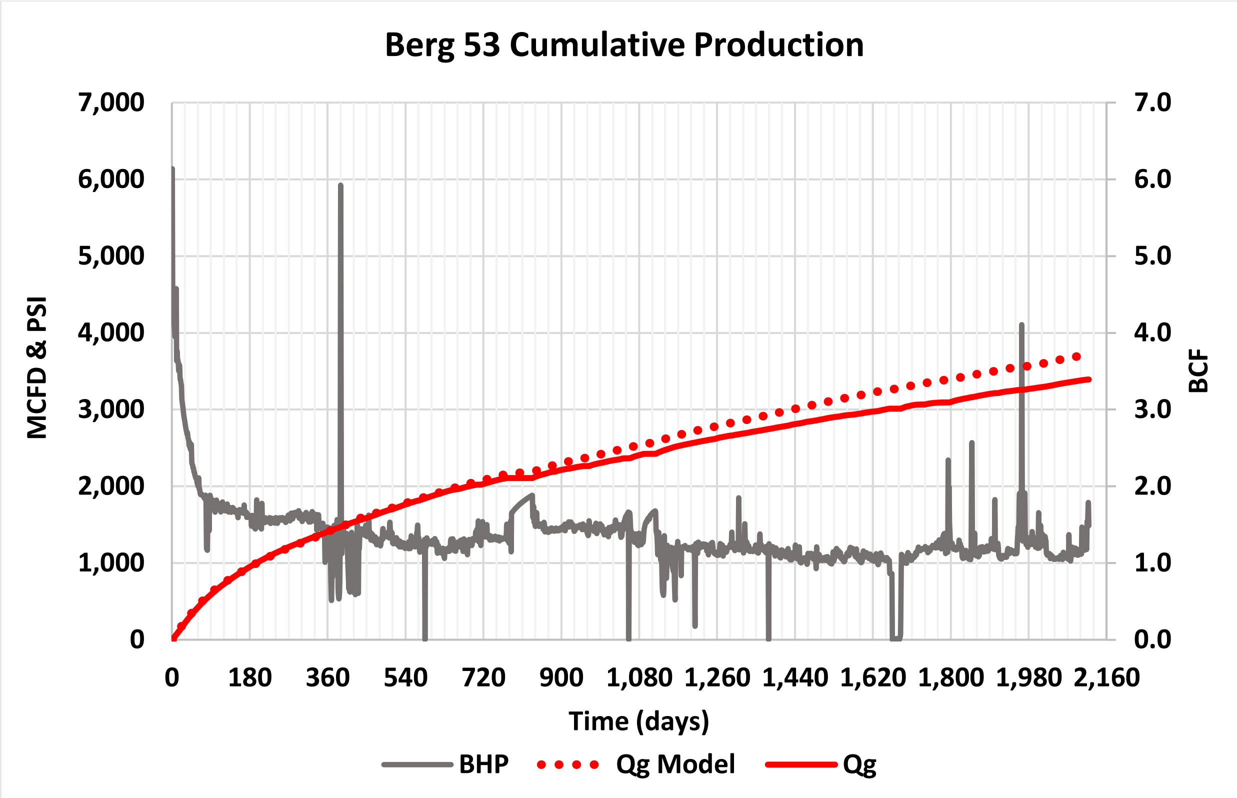

Figure 21 - Match using parameters determined from initial production data assuming each fracture drains a 8:1 channel.

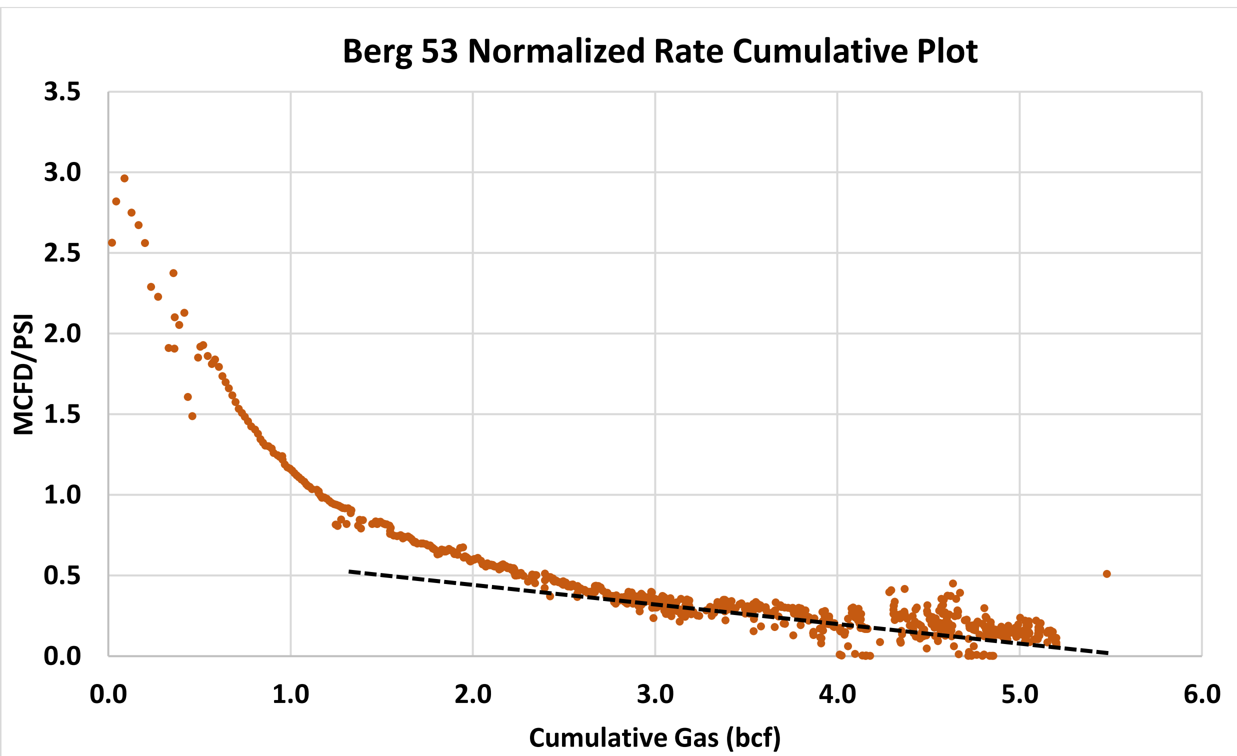

Figure 22 – Normalized Rate Cumulative plot with 6 years of data indicating total contacted volume at 6 years

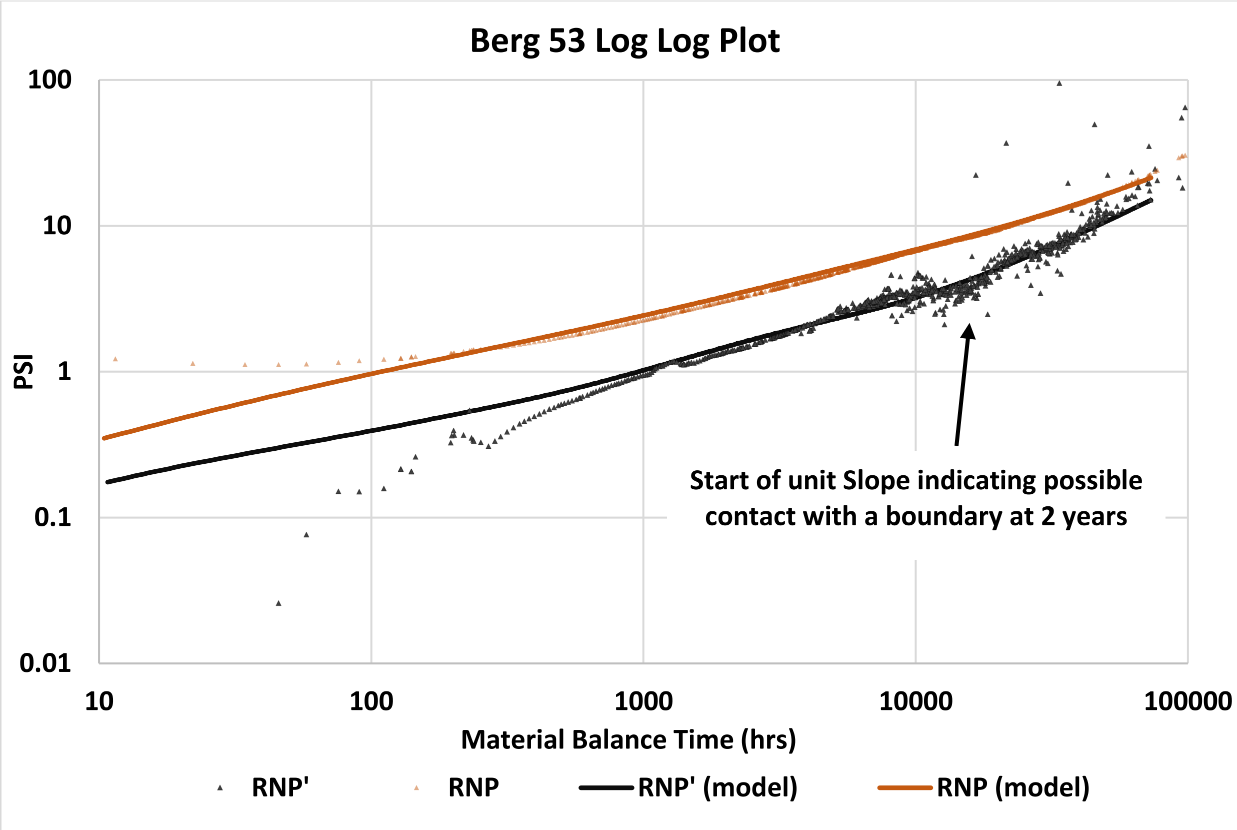

Figure 23 - Log-Log Plot indicating a unit slope starting at 2 years

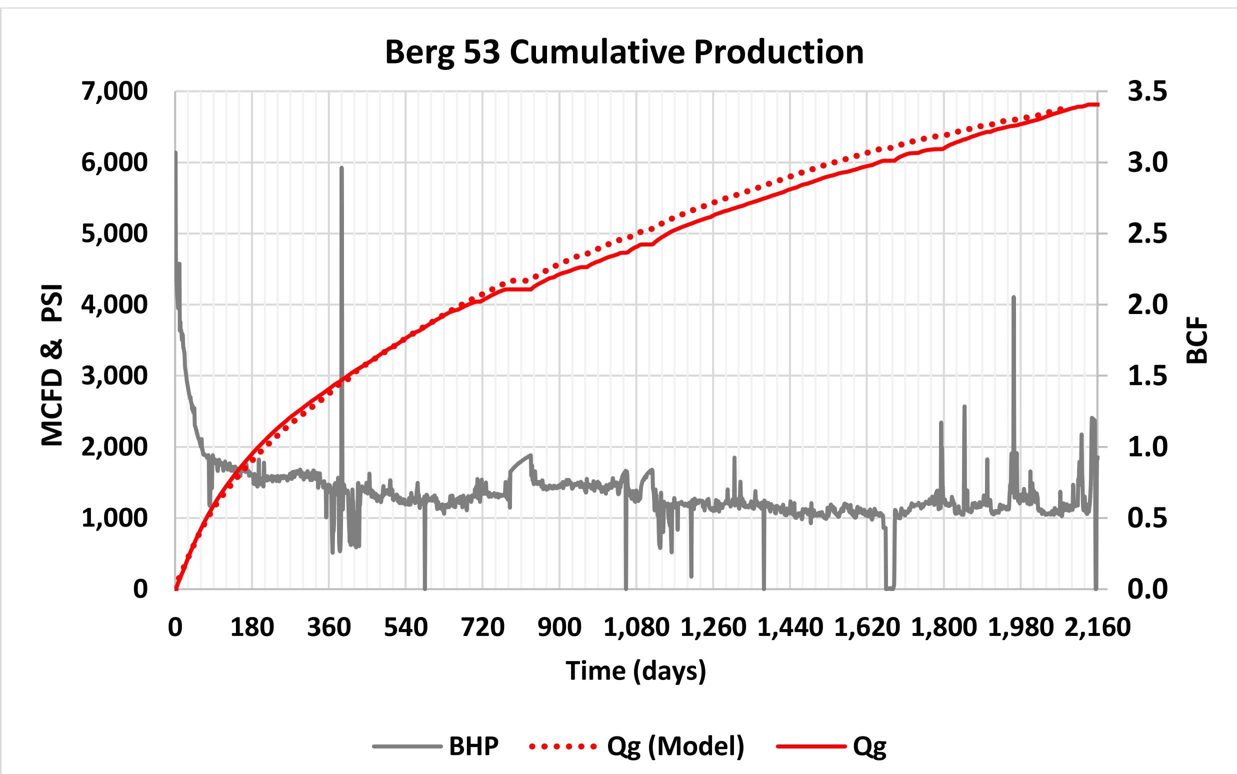

Figure 24 - Production History showing model match constrained with the contacted volume in Figure 20

Oil Example

Well 4 in the SPE Data Repository (BERG) is described as a child well with a modern completion design offsetting a parent well with a legacy completion design in the Eagle Ford. It was completed with 34 stages and 9 clusters per stage. The production history plot is shown in Figure 25.

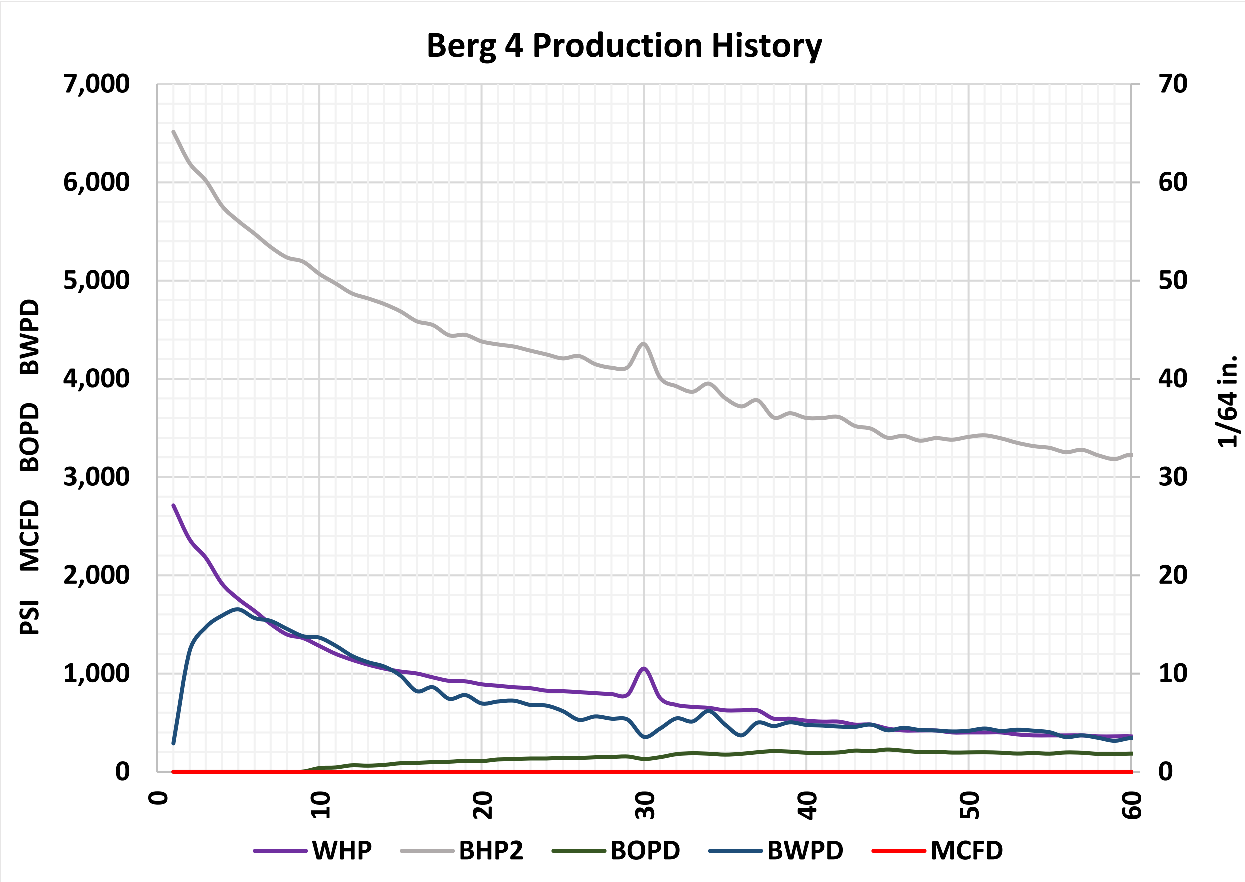

Figure 25 - Oil well example. Production History plot indicating some rate errors

Daily rates and pressures are provided. No hourly rate, pressure or choke data is available. Sand face pressures in the spreadsheet were used as the BHP.

We assume that the choke was being increased until 45 days into the test when peak oil rates were observed. The normalized rate cumulative plot indicates a change in volume after 18 days (Figure 26). However, without hourly rates and pressures and choke data the signatures on the log-log plot that would help to confirm interference cannot be observed. This is especially true for an oil well where transients propagate faster than gas wells due to the lower system compressibility. With faster transient propagation speeds, it's even more important to have accurately measured hourly rates and pressures along with choke data to reduce the uncertainty about when fracture interference occurs.

An extrapolation of the data before the change in volume on the normalized rate cumulative plot gives a volume of 0.16 MMSTb at which fractures started to interfere (Figure 26).

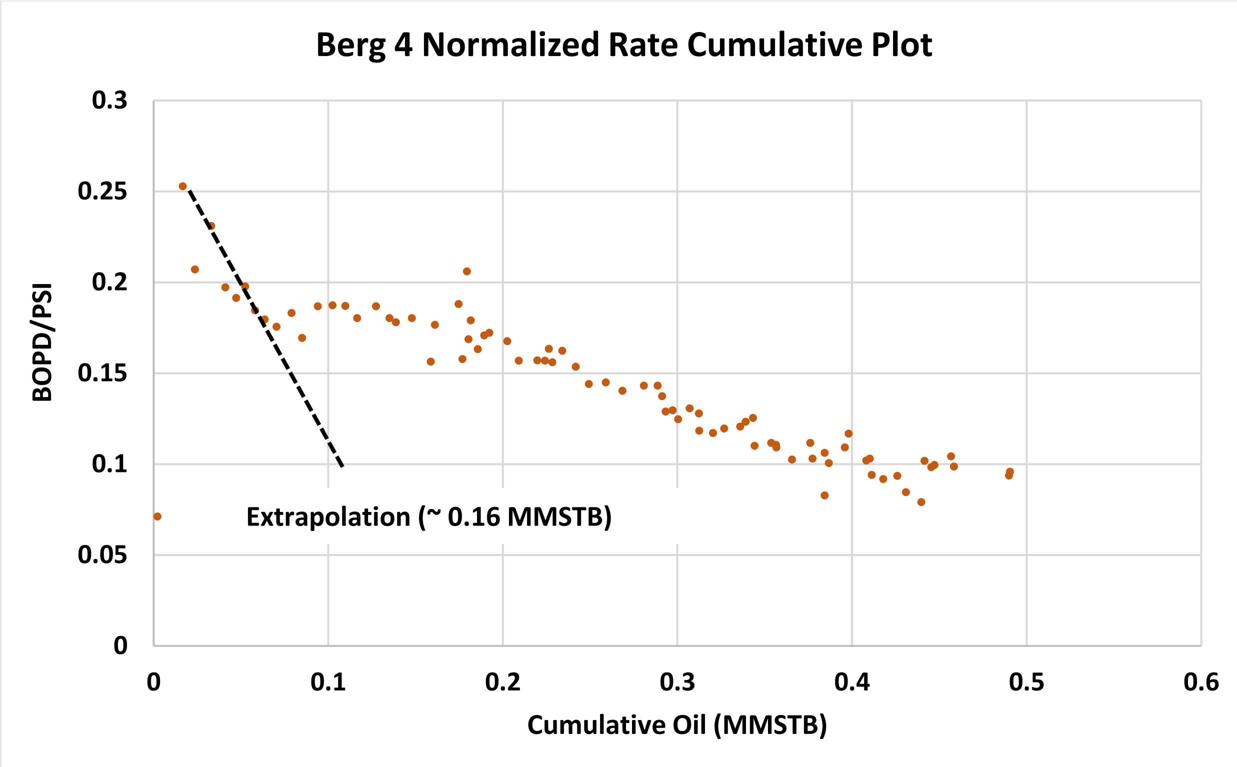

Figure 26 – Extrapolation to determine the volume at first boundary for Berg 4 data (~ 0.16 MMSTB). In contrast with Figure 7 transients associated with choke changes are not visible

The iteration calculation results in an estimated 0.8 fractures/stage (10% cluster efficiency) and a total height of 1,539 ft (Table 5).

Calculations

Volume at interference	160,000	STB
Vb (Bulk volume)	46,309,278	ft3
height/stage	57	ft
# of dominant fractures	27	
re1	97.9	ft
LL	5,086	ft
re2	**97.8**	**ft**
re2-re1	0	ft
Total height	1,539	ft

Table 5 - Calculating the number of dominant fractures for Berg 4H

A model match to the data at 600 hours assuming radial flow (similar to Figure 13) gives a permeability of 0.005 md and a fracture half-length of 90 ft. Seeding the analytical model with this data and adjusting the match results in a permeability of 0.006 md and fracture half-length of 71 ft matching the data. The model match is shown on the log-log plot in Figure 27 and the production history in Figure 28.

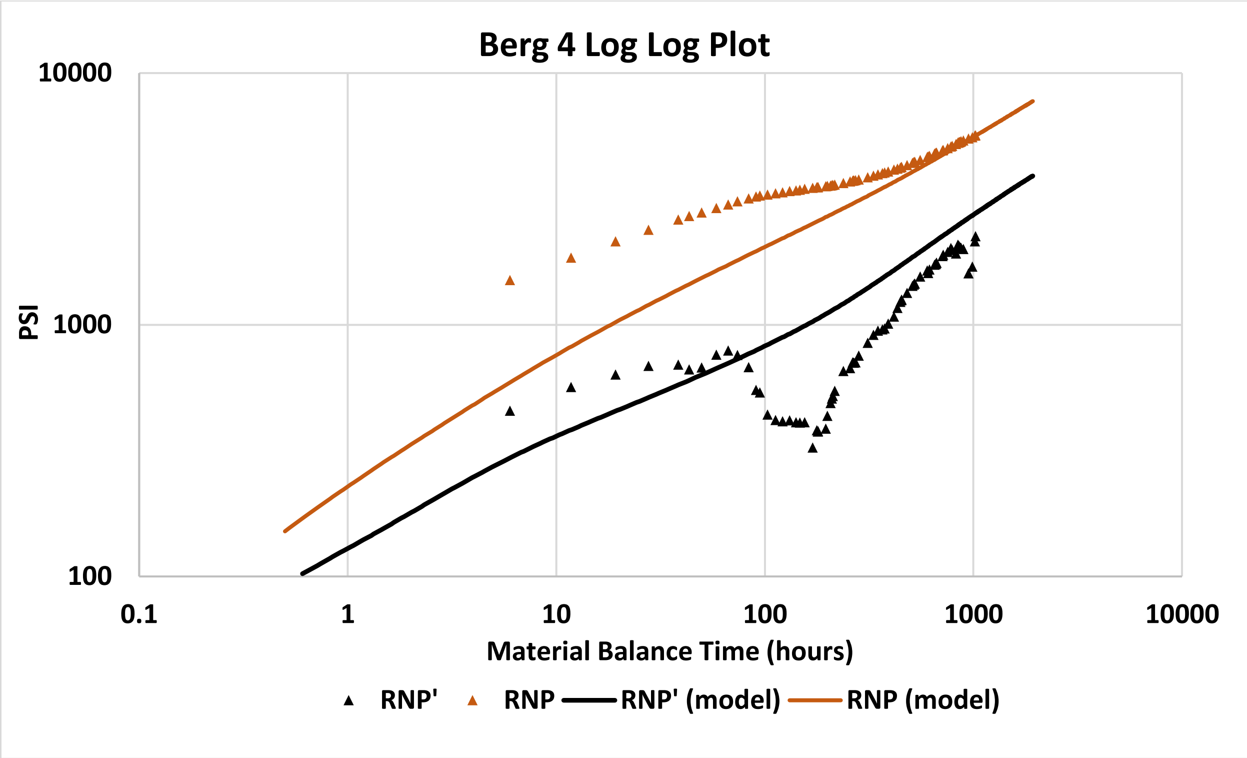

Figure 27 - Log-Log plot of model match to initial production data

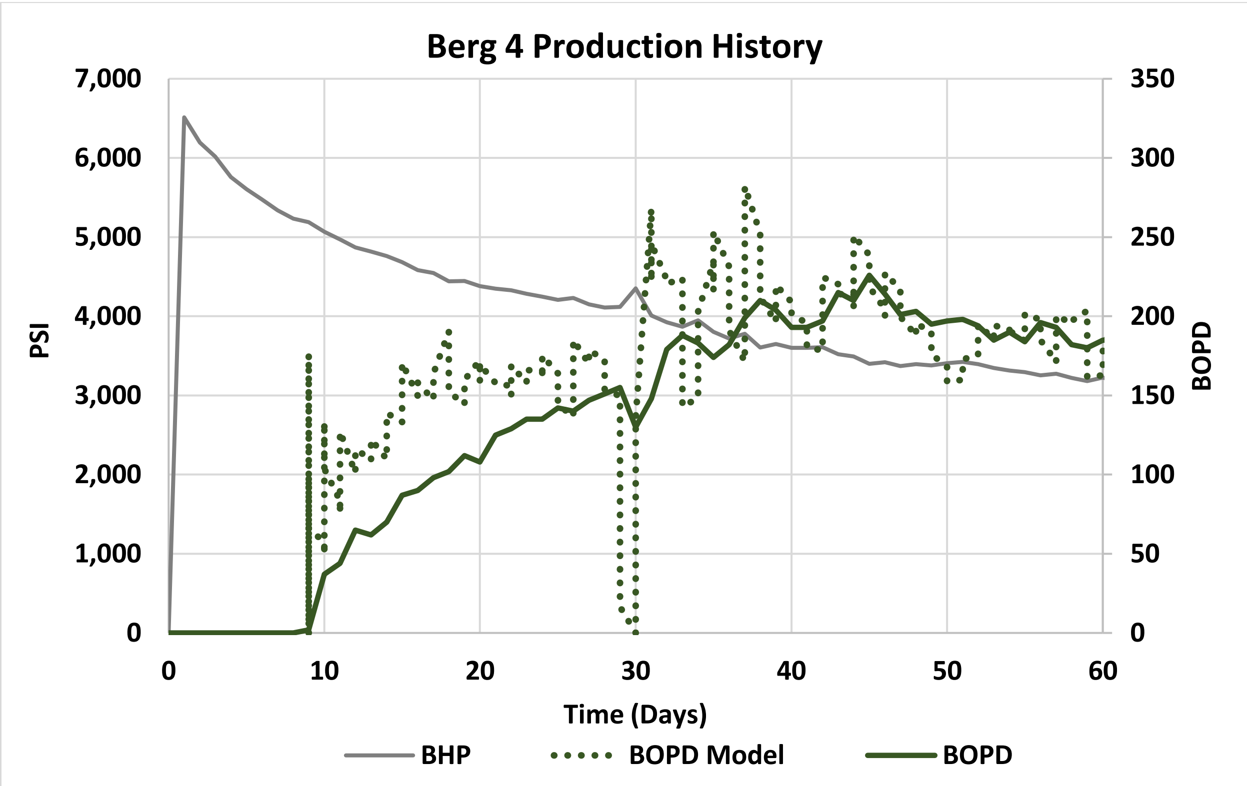

Figure 28 - Model match to first 2 months of data using the fracture half-length and permeability determined using initial production data

The fracture and reservoir parameters determined from the first 60 days are then used to predict production for the next 2.5 years assuming an SRV boundary or offset well interference occurred at 500 ft from the well and using the BHP in the well data. The forecast with initial production data parameters starts to overestimate after 6 months (Figure 29) and is 6% and 16% higher than the actual production after 1.5 and 2.5 years.

With additional data, refinements can be made to this match. The production ratios (not shown) indicate increasing GOR. This indicates that performance may be degrading due to decreasing oil saturation and permeability to oil in the reservoir due to the well flowing pressure dropping below the bubble point and/or interference causing the average reservoir pressure to drop below the bubble point.

The FMB plot in Figure 30 indicates a total system volume of 0.64 MSTB at the same time the log-log plot in figure 31 indicates a boundary (unit slope). From this the outer boundary (assumed to be the boundary between wells) can be calculated and the model rerun with this as a constraint. Figure 32 shows the cumulative production model match once the corrected outer boundary is added to the model. As demonstrated with the previous example (Berg 53) if the distance to the outer boundary is known the entire production history of the well could be modeled.

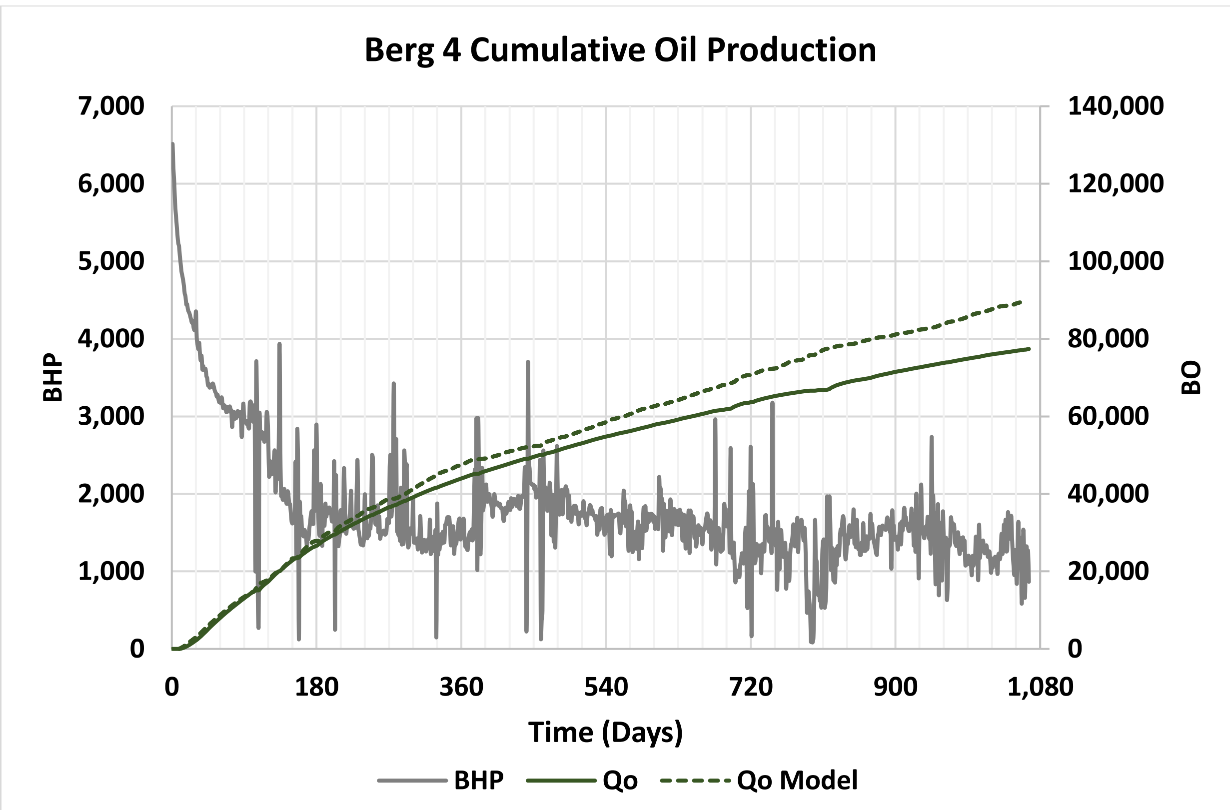

Figure 29 - Cumulative oil comparison between data and model for Berg 4 with no adjustments for boundary effects

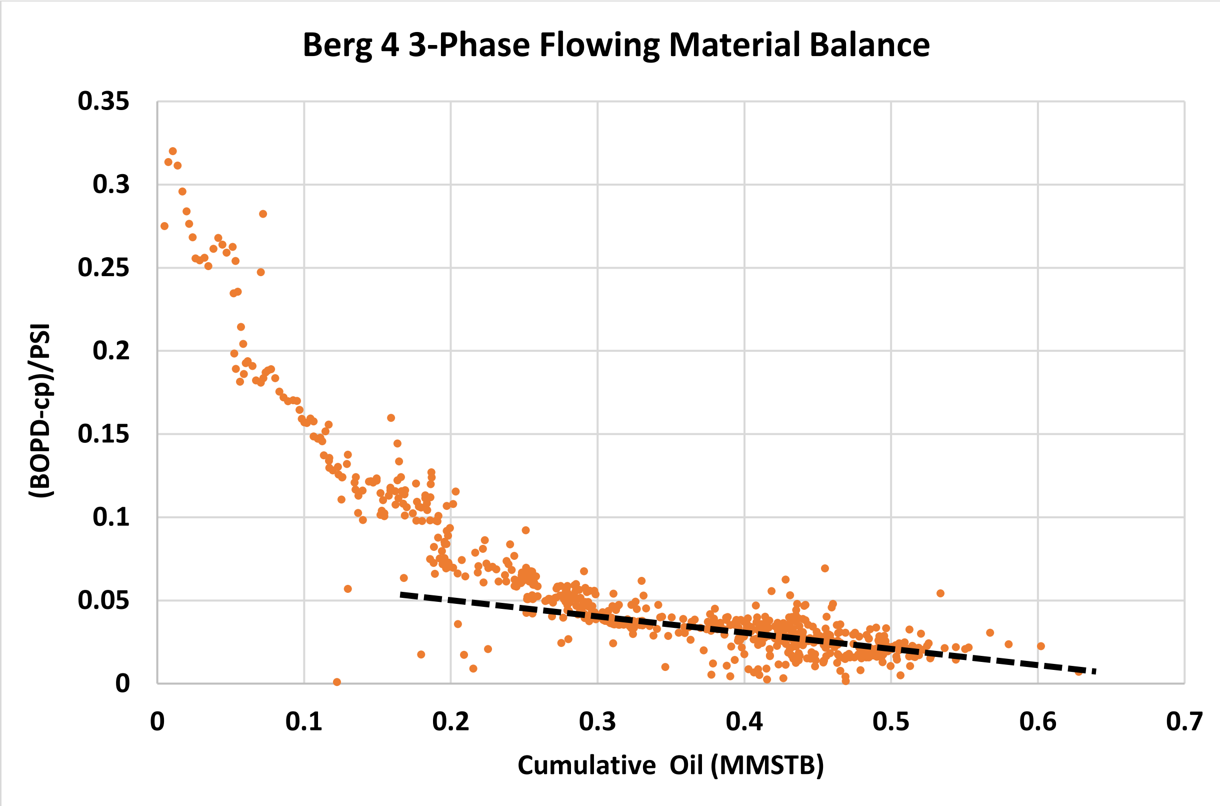

Figure 30 - A slope to the data 2.5 years indicating a volume of 0.64 MMSTB

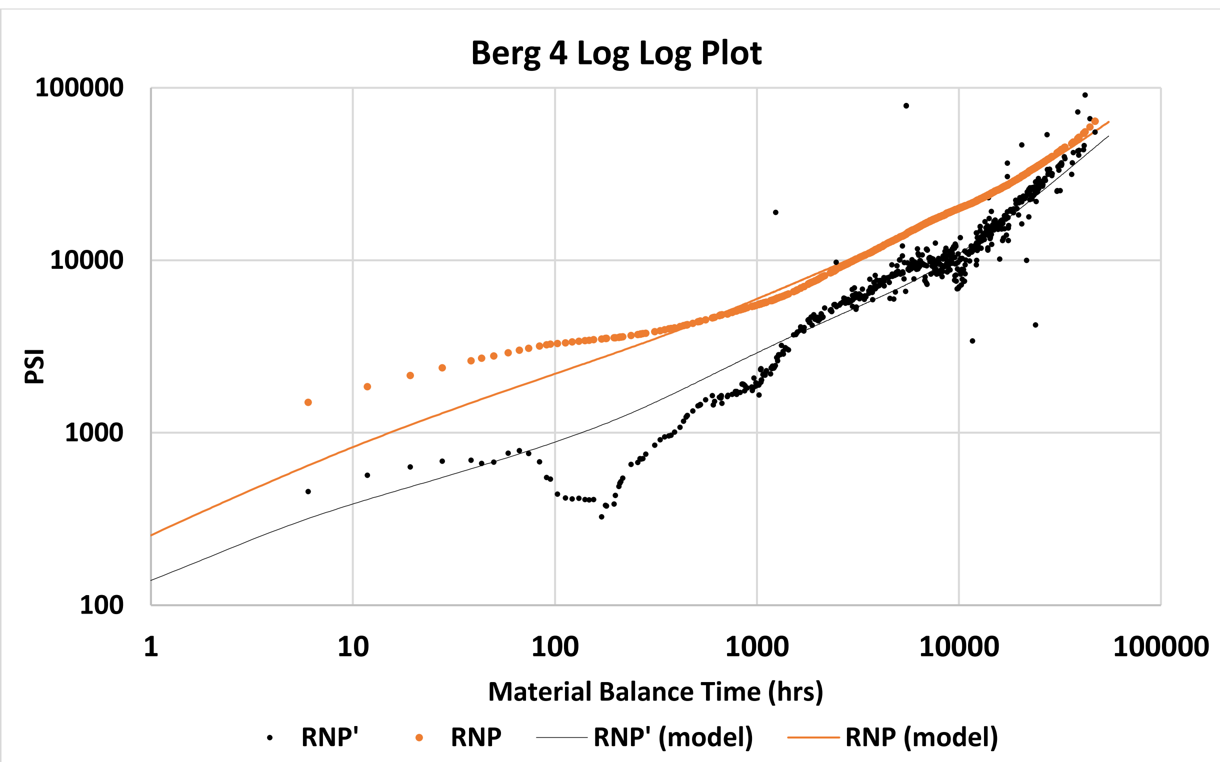

Figure 31 - Log-Log plot of Berg 4 showing the model match rerun with constraints

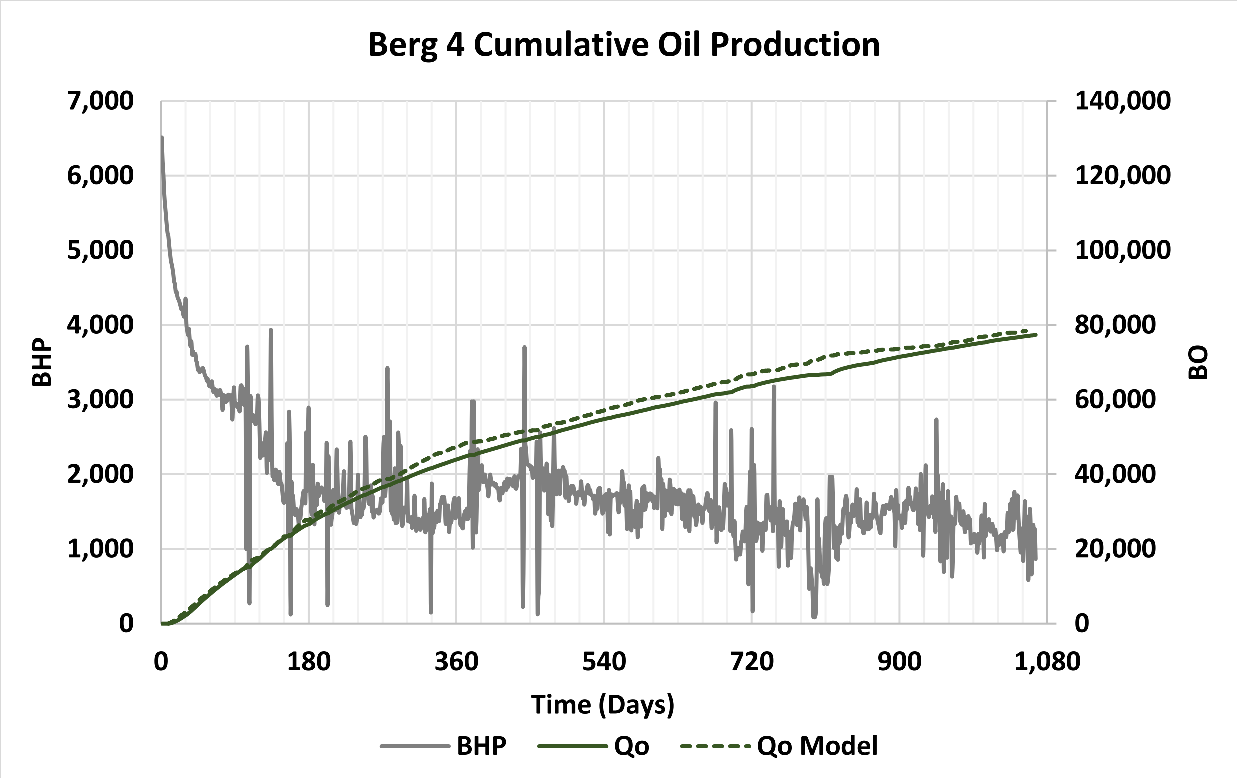

Figure 32 - Log-Log plot and cumulative production plot showing the model match constrained by the contacted volume in Figure 30

Conclusions

1. With the assumption of early facture interference, data from the initial production period was used to determine fracture half-length, permeability, dominant fracture spacing and fractures/stage for 2 wells in the SPE Data Repository.

   A forecast was made with the model match. The cumulative production was matched by the model until a unit slope was observed on log-log plots.

   The modeled cumulative production matched the data when the well geometry was constrained with the volumes contacted by both wells.

2. The crucial insight from this paper is that hourly rate and pressure data (along with choke settings) that is measured accurately during the initial production period (< 2 months of production) captures reservoir transients and helps to diagnose earlier fracture interference than indicated by linear flow analysis.

   Traditional linear flow analysis assumes that fracture interference coincides with the SRV or inter-well boundary. However, the simplified flow regime sequence indicating early interference starts with a boundary between stages / dominant fractures, linear channel flow, and then boundary dominated flow.

3. A numerical model was constructed illustrating the flow regime sequence with early interference, based on data provided from hydraulic fracture test site, which indicates each stage has a couple of dominant fractures with many smaller fractures.

A simplification of this model indicates that the interference observed between the dominant fractures is consistent with the inflection on the derivative of the log-log plot in field data with accurately measured hourly rates, pressures, and choke data.

As illustrated in Figure 3 and 4 a more complicated model may be more physically representative, but the simplified approach has been used to facilitate a consistent workflow for interpreting field data.

4. The analysis method illustrated in this paper using initial production data (within the first 60 days of production) helps predict production when the fracture half-length and permeability don't change significantly from when they were originally assessed. In addition, if the fracture half-length and permeability degrade, or interference occurs the analysis method can help identify the magnitude of lost performance.
5. Daily data can be used for the analysis, however the transients indicating early fracture interference are masked by noisy hourly data and daily data or data with significant operational upsets. Hourly, high-quality data reduces uncertainty in the analysis.

References

Alexander C. Eleiott, W. J. 2019. Modified Fetkovich Type Curve Enhances Type Well Construction for Horizontal Wells with Multiple Fractures. Presented at the Unconventional Resources Technology Conference. Denver, Colorado, 22-24 July. URTeC 2019-471. https://doi.org/10.15530/urtec-2019-471

Alzahabi, A., Trindade, A. A., Kamel, A. A., Harouaka, A., Baustian, W., & Campbell, C. 2021. Optimal Drawdown for Woodford and Mayes in the Anadarko Basin Using Data Analytics. SPE Prod & Oper, 36(03), 572–582. SPE-201660-PA. https://doi.org/10.2118/201660-PA

Anderson, D. M., Nobakht, M., Moghadam, S., & Mattar, L. (2010). Analysis of Production Data from Fractured Shale Gas Wells. Presented at the SPE Unconventional Gas Conference. October 19–21, 2010. Pittsburgh, Pennsylvania, USA: SPE-137755-MS. https://doi.org/10.2118/137755-MS

Aniemena, C., LaMarca, C., & Labryer, A. (2019). Well Spacing Optimization in Shale Reservoirs Using Rate Transient Analytics. Presented at the SPE/AAPG/SEG Unconventional Resources Technology Conference, Denver, Colorado, USA, July 22–24, 2019. URTEC-2019-278 MS https://doi.org/10.15530/urtec-2019-278

Barree, R. D. 2019. Fracture Conductivity and Clean Up in Gohfer Software.

Barree, R. D., Cox, S. A., Miskimins, J. L., Gilbert, J. V., & Conway, M. W. (2015). Economic Optimization of Horizontal-Well Completions in Unconventional Reservoirs. SPE Prod & Oper, 30 ()4), 293–311. SPE-168612-PA. https://doi.org/10.2118/168612-PA

Barree, R. D., Duenckel, R. J., & Hlidek, B. T. 2019. The Limits of Fluid Flow in Propped Fractures- the Disparity Between Effective Flowing and Created Fracture Lengths. Presented at the SPE Hydraulic Fracturing Technology Conference and Exhibition. The Woodlands, Texas, USA, 5-7 February 2019. SPE-194355-MS. https://doi.org/10.2118/194355-MS

Belyadi, H., Fathi, E., & Belyadi, F. 2016. Managed Pressure Drawdown in Utica/Point Pleasant with Case Studies. Presented at the SPE Eastern Regional Meeting, Canton. Ohio, USA. September 13–15, 2016. SPE-184054-MS. https://doi.org/10.2118/184054-MS

BERG. SPE Data Repository. Retrieved 04/14/2022. https://www.spe.org/en/industry/data-repository/

Bessa, F., Jerath, K., Ginn, C., Johnston, P., Zhao, Y., Brown, T., . . . Sahni, V. 2021. Subsurface Characterization of Hydraulic Fracture Test Site-2 (HFTS-2), Delaware Basin. Presented at the SPE/AAPG/SEG Unconventional Resources Technology Conference, Houston, Texas, USA. July 26–28, 2021. URTEC-2021-5243-MS. https://doi.org/10.15530/urtec-2021-5243

Burget, B., Dannemiller, N., Garrett, D., & Kling, E. 2021. Optimizing Completion Design and Well Spacing in the Powder River Basin Niobrara Oil Play. Presented at the SPE Hydraulic Fracturing Technology Conference and Exhibition, Virtual, May 4–6, 2021: SPE-204167-MS. https://doi.org/10.2118/204167-MS

Crafton, J. W. 1998. Well Evaluation Using Early Time Post-Stimulation Flowback Data. Presented at the SPE Annual Technical Conference and Exhibition, New Orleans, Louisiana. September 27–30, 1998. SPE-49223-MS. https://doi.org/10.2118/49223-MS

Crafton, J. W. 2008. Modeling Flowback Behavior or Flowback Equals "Slowback". Presented at the SPE Shale Gas Production Conference. Fort Worth, Texas, USA: November 16–18, 2008. SPE-119894-MS. https://doi.org/10.2118/119894-MS

Deen, T., Daal, J., & Tucker, J. 2015. Maximizing Well Deliverability in the Eagle Ford Shale Through Flowback Operations. Presented at the SPE Annual Technical Conference and Exhibition. Houston, Texas, USA, September 28–30, 2015. SPE-174831-MS. https://doi.org/10.2118/174831-MS

Fowler, G., McClure, M., & Cipolla, C. 2019. A Utica Case Study: The Impact of Permeability Estimates on History Matching, Fracture Length, and Well Spacing. Presented at the SPE Annual Technical Conference and Exhibition, September 30–October 2, 2019. Calgary, Alberta: SPE-195980-MS. https://doi.org/10.2118/195980-MS

Lee, J., Rollins, J. B., & Spivey, J. P. (2003). Pressure Transient Testing. Richardson, Texas. Society of Petroleum Engineers.

Lemoine, R., & Lee, J. 2019. Integrated Workflow Reduces Uncertainty in Type Well Construction and Production Forecasting of Multi-Fractured Horizontal Wells. Presented at the SPE Western Regional Meeting. San Jose, California, USA. April 23–26, 2019. SPE-195281-MS https://doi.org/10.2118/195281-MS

Lerza, A., Rojas, D., & Liang, B. 2018. Defining the Optimal Drawdown Strategy in the Vaca Muerta Formation. Presented at the Unconventional Resources Technology Conference. Houston, Texas, USA. July 23–25, 2018. URTEC-2880115-MS. https://doi.org/10.15530/URTEC-2018-2880115

Nobakht, M., Clarkson, C. R., & Kaviani, D. 2011. New Type Curves for Analyzing Horizontal Well with Multiple Fractures in Shale Gas Reservoirs. Presented at the Canadian Unconventional Resources Conference. Calgary, Alberta, Canada, November 2011: SPE-149397-MS https://doi.org/10.2118/149397-MS

Okouma, V., Guillot, F., Sarfare, M., Sen, V., Ilk, D., & Blasingame, T. A. 2011. Estimated Ultimate Recovery (EUR) as a Function of Production Practices in the Haynesville Shale. Presented at the SPE

Annual Technical Conference and Exhibition, Denver, Colorado, USA. October 30–November 2, 2011. SPE-147623-MS. https://doi.org/10.2118/147623-MS

Olivier Houze, D. V. 2021. Dynamic Data Analysis. Kappa.

P.W. Collins, D. Ilk.2015. Practical Considerations for Production Forecasting in Unconventional Reservoir Systems — Processing of Large Group of Wells Using Production Diagnostics and Model-Based Analysis. Presented at the SPE Annual Technical Conference and Exhibition. Houston. September 28–30, 2015. SPE-174984-MS. https://doi.org/10.2118/174984-MS

Raterman, K., Liu, Y., Roy, B., Friehauf, K., Thompson, B., & Janssen, A. 2020. Analysis of a Multi-Well Eagle Ford Pilot. Presented at the SPE/AAPG/SEG Unconventional Resources Technology Conference. Virtual. July 20–22, 2020. URTEC-2020-2570-MS. https://doi.org/10.15530/urtec-2020-2570

Ravikumar, A., & Lee, W. J. 2020. Model-based Type Wells Reduce Uncertainty in Production Forecasting For Unconventional Wells. Presented at the SPE/AAPG/SEG Unconventional Resources Technology Conference, Virtual. July 20–22, 2020 Austin. URTEC-2020-3245-MS. https://doi.org/10.15530/urtec-2020-3245

Rojas, D., & Lerza, A. 2018. Horizontal Well Productivity Enhancement through Drawdown Management Approach in Vaca Muerta Shale. Presented at the SPE Canada Unconventional Resources Conference. Calgary, Alberta, Canada, March 2018. SPE-189822-MS. https://doi.org/10.2118/189822-MS

Sukumar, S., & Lee, W. J. 2019. Type Wells – A Physics-Blind Statistical Myth? Our RTA Driven Construction Methodology Proves Otherwise! Presented at the SPE Western Regional Meeting. San Jose, California: SPE. July 2021. URTEC-2021-5030-MS. https://doi.org/10.15530/urtec-2021-5030

Tompkins, D., Kerls, M., & Adejare, O. 2020. An Examination of the Effects of Surface Data Acquisition Methods on Well Performance Evaluations and Completion Optimization. Presented at the SPE/AAPG/SEG Unconventional Resources Technology Conference. Virtual, July 2020. URTEC-2020-2515-MS. https://doi.org/10.15530/urtec-2020-2515

Tompkins, D., Kerls, M., & Adejare, O. 2021. Automated Well Performance Diagnostics in Unconventional Reservoirs: A Multi Basin Study for Early Time Production Optimization. Presented at the SPE/AAPG/SEG Asia Pacific Unconventional Resources Technology Conference. Virtual. URTEC-208282-MS. https://doi.org/10.15530/AP-URTEC-2021-208282

Tompkins, D., Sieker, R., Koseluk, D., & Cartaya, H. 2016. Managed Pressure Flowback in Unconventional Reservoirs: A Permian Basin Case Study. Presented at the SPE/AAPG/SEG Unconventional Resources Technology Conference. San Antonio, Texas, USA. August 2016. URTEC-2461207-MS. https://doi.org/10.15530/URTEC-2016-2461207

Whitson Academy. (2022) Whitson Webinar - Linking Multiphase Flowing Material Balance method to Recovery Factor Calculations. Retrieved 04/12/2022, from https://www.youtube.com/watch?v=l6YKzzMykqY